2

3   Bin Wang[1], Michela Biasutti[2], Michael P. Byrne[3,4], Christopher Castro[4], Chih-Pei Chang[5,6], Kerry

4   Cook[7], Rong Fu[8], Alice M. Grimm[9], Kyung-Ja Ha[10,11,12], Harry Hendon[13], Akio Kitoh[14,15], R.

5   Krishnan[16], June-Yi Lee[11,12], Jianping Li[17,18], Jian Liu[19], Aurel Moise[20], Salvatore Pascale[21], M. K.

6   Roxy[16], Anji Seth[22], Chung-Hsiung Sui[6], Andrew Turner[23,24], Song Yang[25,26], Kyung-Sook Yun[11],

7   Lixia Zhang[27], Tianjun Zhou[27]

8

9   [1] Department of Atmospheric Sciences, University of Hawaii, Honolulu, HI, USA

10   [2] Lamont-Doherty Earth Observatory, Columbia University, Palisades, NY, USA

11   [3] School of Earth & Environmental Sciences, University of St Andrews, St. Andrews, UK

12   [4] Department of Physics, University of Oxford, Oxford, UK

13   [4] Department of Hydrology and Atmospheric Sciences, University of Arizona, Tucson, AZ, USA

14   [5] Department of Meteorology, Naval Postgraduate School, Monterey, CA, USA

15   [6] Department of Atmospheric Sciences, National Taiwan University, Taipei, Taiwan

16   [7] Department of Geological Sciences, University of Texas, Austin, TX, USA

17   [8] Department of Atmospheric and Oceanic Sciences, University of California, Los Angeles, CA,

18   USA

19   [9] Department of Physics, Federal University of Paraná, Curitiba, Brazil

20   [10] Department of Atmospheric Sciences, Pusan National University, Busan, Republic of Korea

21   [11] Institute for Basic Science, Center for Climate Physics, Busan, Republic of Korea

22   [12] Research Center for Climate Sciences and Department of Climate System, Pusan National

23   University, Busan, Republic of Korea

24   [13] Bureau of Meteorology, Melbourne, Australia

25   [14] Japan Meteorological Business Support Center, Tsukuba, Japan

26   [15] Meteorological Research Institute, Tsukuba, Japan

27   [16] Indian Institute of Tropical Meteorology, Pune, India

28   [17] Institute for Advanced Ocean Studies, Ocean University of China, Qingdao, China

29   [18] Pilot Qingdao National Laboratory for Marine Science and Technology, China

30   [19] School of Geographic and Oceanographic Sciences, Nanjing Normal University, Nanjing, China

31   [20] Center for Climate Research Singapore, Republic of Singapore

32   [21] Department of Earth System Sciences, Stanford University, Stanford, CA, USA

33   [22] Department of Geography, University of Connecticut, Storrs, CT, USA

34   [23] Department of Meteorology, University of Reading, Reading, UK

35   [24] National Centre for Atmospheric Science, University of Reading, Reading, UK

36   [25] School of Atmospheric Sciences and Guangdong Province Key Laboratory for Climate Change

37   and Natural Disaster Studies, Sun Yat-sen University, Guangzhou, China

38   [26] Southern Marine Science and Engineering Guangdong Laboratory (Zhuhai), China

39   [27] Institute of Atmospheric Physics, Chinese Academy of Sciences, China

40

41

42

43   Corresponding Author: Dr. Chih-Pei Chang, email:cpchang@nps.edu

44

2

45

46   Abstract

47   Monsoon rainfall has profound economic and societal impacts for more than two-thirds of the

48   global population. Here we provide a review on past monsoon changes and their primary

49   drivers, the projected future changes and key physical processes, and discuss challenges of the

50   present and future modeling and outlooks. Continued global warming and urbanization over

51   the past century has already caused a significant rise in the intensity and frequency of extreme

52   rainfall events in all monsoon regions (high confidence). Observed changes in the mean

53   monsoon rainfall vary by region with significant decadal variations. NH land monsoon rainfall as

54   a whole declined from 1950 to 1980 and rebounded after the 1980s, due to the competing

55   influences of internal climate variability and radiative forcing from GHGs and aerosol forcing

56   (high confidence); however, it remains a challenge to quantify their relative contributions.

57   The CMIP6 models simulate better global monsoon intensity and precipitation over CMIP5

58   models, but common biases and large intermodal spreads persist. Nevertheless, there is high

59   confidence that the frequency and intensity of monsoon extreme rainfall events will increase,

60   alongside an increasing risk of drought over some regions. Also, land monsoon rainfall will

61   increase in South Asia and East Asia (high confidence) and northern Africa (medium confidence),

62   and decrease in North America and unchanged in Southern Hemisphere. Over Asian-Australian

63   monsoon region the rainfall variability is projected to increase on daily to decadal scales. The

64   rainy season will likely be lengthened in the Northern Hemisphere due to late retreat

65   (especially over East Asia), but shortened in the Southern Hemisphere due to delayed onset.

66

67

68   Capsule Summary

69   This paper reviews the current knowledge on detection, attribution and projection of global

70   and regional monsoons (South Asian, East Asian, Australian, South American, North American,

71   and African) under climate change.

72

1. Introduction

Many parts of the Earth's surface and two-thirds of the global population are influenced by the monsoon. This paper reviews the current state of knowledge of climate change and its impacts on the global monsoon and its regional components, including recent results from phase six of the Coupled Model Intercomparison Project (CMIP6) that were reported at a World Meteorological Organization/World Weather Research Programme workshop held in Zhuhai in early December 2019. The review's primary focus is on monsoon rainfall, both mean and extremes, whose variability has tremendous economic and societal impacts. Due to the large body of literature on this broad topic, only a fraction can be cited in this concise review.

The global monsoon (GM) is a defining feature of the Earth's climate and a forced response of the coupled climate system to the annual cycle of solar insolation. For clarity, we define the monsoon domain primarily based on rainfall contrast in the solstice seasons (Fig. 1). The North American monsoon (NAM) domain covers western Mexico and Arizona, but also Central America and Venezuela, and is larger than that traditionally recognized by many scientists working on the NAM. We aim to encompass the range of literature marrying together global monsoon, regional monsoon and paleoclimate monsoon perspectives and therefore reach a compromise. Equatorial Africa and the Maritime Continent also feature annual reversal of surface winds, although the former has a double peak in the equinoctial seasons and the latter is heavily influenced by complex terrain (Chang 2004).

Our goal is to outline past changes of the monsoon and identify the key drivers of these changes, assess the roles and impacts of natural and anthropogenic forcings and regional variability, and discuss the limitations and difficulties of current climate models in representing

5

95   monsoon variability. We will also attempt to summarize projected future changes both globally

96   and in various monsoon regions using recent model results. Due to the inherent uncertainties

97   and model limitations, the degree of confidence in the results varies. A section on model issues

98   and outlook is devoted to discussing challenges of present and future monsoon modeling.

99   **2. Global monsoon**

100   2.1. Detection and Attribution of observed changes

101   Wang and Ding (2006) found a decreasing trend of global land monsoon precipitation

102   from the 1950s to 1980, mainly due to the declining monsoon in the northern hemisphere (NH).

103   After 1980, GM precipitation (GMP) has intensified due to a significant upward trend in the NH

104   summer monsoon (Wang et al., 2012). Extended analysis of the whole 20th century NH land

105   monsoon rainfall indicates that short-period trends may be part of multidecadal variability,

106   which is primarily driven by forcing from the Atlantic (Atlantic Multidecadal Variation; AMV,

107   and the Pacific (Interdecadal Pacific Oscillation; IPO) (Zhou et al. 2008, Wang et al. 2013, 2018;

108   Huang et al. 2020a). On the other hand, there is evidence that anthropogenic aerosols have

109   influenced decreases of NH land monsoon precipitation in the Sahel, South and East Asia during

110   the second half of the 20th century (Polson et al., 2014; Giannini and Kaplan, 2019; Zhou et al.,

111   2020b). It should be noted that this long-term decrease in precipitation could be, in part, due to

112   natural multi-decadal variations of the regional monsoon precipitation (Sontakke et al. 2008, Jin

113   and Wang 2017; Huang et al., 2020b). It remains a major challenge, however, to quantify the

114   relative contributions of internal modes of variability versus anthropogenic forcing on the

115   global scale.

116   2.2. Projected long-term changes

6

117   The CMIP5 results suggest that GM area, annual range and mean precipitation are likely

118   to increase by the end of the 21st century (Kitoh et al., 2013; Hsu et al., 2013; Christensen et al.,

119   2013). The increase will be stronger in the NH, and the NH rainy season is likely to lengthen due

120   to earlier or unchanged onset dates and a delayed retreat (Lee and Wang, 2014). The increase

121   in GM precipitation was primarily attributed to temperature-driven increases in specific

122   humidity, resulting in the "wet-get-wetter" pattern (Held and Soden, 2006).

123   Analysis of 34 CMIP6 models indicates a larger increase in monsoon rainfall over land

124   than over ocean in all four core Shared Socio-economic Pathways (SSPs) (Fig. 2; Lee et al. 2019).

125   The projected GMP increase over land by the end of the 21st century relative to 1995-2014 in

126   CMIP6 is about 50% larger than in CMIP5. Models with high (>4.2°C) equilibrium climate

127   sensitivity (ECS) account for this larger projection. The causes of CMIP6 models' high ECS has

128   been discussed in Zelinka et al. (2020). Note that the forced signal of GMP over land shows a

129   decreasing trend from 1950 to the 1980s, but the trend reversed around 1990, which is

130   consistent with the CMIP5 results (Lee and Wang, 2014). During 1950-1990, the temperature-

131   driven intensification of precipitation was likely masked by a fast precipitation response to

132   anthropogenic sulfate and volcanic forcing, even though the warming trend due to GHG since

133   the pre-industrial period (1850-1900) is three times larger than the cooling due to aerosol

134   forcing (Lau and Kim, 2017; Richardson et al. 2018;). The recent upward trend may signify the

135   emergence of the greenhouse-gas signal against the rainfall reduction due to aerosol emissions.

136   However, the trend during recent decades can be influenced by the leading modes of

137   multidecadal variability of global SST (Wang et al. 2018). Lee et al. (2019) found that land

138   monsoon precipitation sensitivity (precipitation change per degree of global warming) slightly

7

139   increases with the level of GHG forcing, whereas the ocean monsoon precipitation has almost

140   no sensitivity (Fig. 2). The GM land precipitation sensitivity has a median of 0.8 %/°C in SSP2-4.5,

141   and a median of 1.4%/°C in SSP5-8.5. The latter is slightly higher than that simulated by CMIP5

142   models under RCP 8.5.

143   Wang et al. (2020) examined the ensemble-mean projection from 15 early-released

144   CMIP6 models, which estimates that under SSP2-4.5 the total NH land monsoon precipitation

145   will increase by about 2.8%/°C in contrast to little change in the southern hemisphere (SH; -

146   0.3%/°C). In both hemispheres, the annual range of land monsoon rainfall will increase by

147   about 2.6%/°C, with wetter summers and drier winters. In addition, the projected land

148   monsoon rainy season will be lengthened in the NH (by about ten days) due to late retreat, but

149   will be shortened in the SH due to delayed onset; the interannual variations of GMP will be

150   more strongly controlled by ENSO variability (Wang et al. 2020). In monsoon regions, increases

151   in specific humidity are spatially uniform (Fig. 4b), but the rainfall change features a robust NH-

152   SH asymmetry and an east-west asymmetry between enhanced Asian-African monsoons and

153   weakened NAM (Fig. 4a), suggesting that circulation changes play a crucial role in shaping the

154   spatial patterns and intensity of GM rainfall changes (Wang et al. 2020). GHG-induced

155   horizontally differential heating results in a robust "NH-warmer-than-SH" pattern (Fig. 4c),

156   which enhances NH monsoon rainfall (Liu et al. 2009, Mohtadi et al. 2016), especially in Asia

157   and northern Africa, due to an enhanced thermal contrast between the large Eurasia-Africa

158   landmass and adjacent oceans (Endo et al. 2018). Those CMIP models that project a stronger

159   inter-hemispheric thermal contrast generate stronger Hadley circulations, more northward

160   positions of the ITCZ, and enhanced NH monsoon precipitation (Wang et al. 2020). The GHG

8

161   forcing also induces a warmer equatorial eastern Pacific (Fig. 4c), which reduces NAM rainfall by

162   shifting the ITCZ equatorward (Wang et al. 2020). Climate models on average predict

163   weakening ascent under global warming (Endo and Kitoh, 2014), which tends to dry monsoon

164   regions. Weakening monsoon ascent has been linked to the slowdown of the global overturning

165   circulation (Held and Soden 2006). However, a definitive theory for why monsoon circulations

166   broadly weaken with warming remains elusive.

167   Land monsoon rainfall (LMR) provides water resources for billions of people; an

168   accurate prediction of its change is vital for the sustainable future of the planet. Regional land

169   monsoon rainfall exhibits very different sensitivities to climate change (Fig. 3). The annual mean

170   LMR in the East Asian and South Asian monsoons shows large positive sensitivities with means

171   of 4.6%/°C, and 3.9%/°C, respectively, under SSP2-4.5. The LMR likely increases in NAF, but

172   decreases in NAM, and remains unchanged in the Southern Hemisphere monsoons (Jin et al.

173   2020).

174   2.3. Projected near-term change

175   The interplay between internal modes of variability, such as IPO, AMV and SH Annular

176   Mode (Zheng et al. 2014), and anthropogenic forcing is important in the historical record and

177   for the near-term future (Chang et al. 2014). Huang et al. (2020a) used two sets of initial

178   condition large ensembles to suggest that internal variability linked to the IPO could overcome

179   the forced upward trend in the South Asian monsoon rainfall up to 2045. Using 20th-century

180   observations and numerical experiments, Wang et al. (2018) showed that the hemispheric

181   thermal contrast in the Atlantic and Indian Oceans and the IPO can be used to predict the NH

182   land monsoon rainfall change a decade in advance. The significant decadal variability of

9

183   monsoon rainfall leads to considerable uncertainties in climate projections for the next 30 years;

184   thus, improvements in predicting internal modes of variability could reduce uncertainties in

185   near-term climate projections.

186   **3. Regional monsoon changes**

187   3.1 South Asian monsoon

188   The South Asian summer monsoon (SASM) circulation experienced a significant

189   declining trend from the 1950s together with a weakening local meridional circulation and

190   notable precipitation decreases over north-central India and the west coast that are associated

191   with a reduced meridional temperature gradient (e.g., Krishnan et al., 2013, Roxy et al. 2015).

192   This trend was attributed to effects of anthropogenic aerosol forcing (e.g., Salzmann et al., 2014;

193   Krishnan et al. 2016) and equatorial Indian Ocean warming due to increased GHG (e.g.,

194   Sabeerali and Ajayamohan 2017). However, it could potentially be altered by multidecadal

195   variations (Shi et al. 2018) arising from internal modes of climate variability such as the IPO and

196   AMV (e.g., Krishnan and Sugi, 2003, Salzmann and Cherian, 2015, Jiang and Zhou 2019). The

197   processes by which aerosols affect monsoons were reviewed by Li et al. (2015). Aerosols can

198   also have a remote impact on regional monsoons (Shaeki et al., 2018).

199   CMIP models consistently project increases in the mean and variability of SASM

200   precipitation, despite weakened circulation at the end of the 21st century relative to the

201   present (e.g., Kitoh et al. 2013; Wang et al. 2014), though some models disagree (Sabeerali and

202   Ajayamohan 2017). The uncertainty in radiative forcing from aerosol emissions in CMIP5 causes

203   a large spread in the response of SASM rainfall (Shonk et al., 2019). However, this is not the

204   case in CMIP6 projections (Fig. 3).

205   3.2 East Asian monsoon

206   During the 20th century, East Asian summer monsoon (EASM) exhibited considerable

207   multi-decadal variability with a weakened circulation and a south flood-north drought pattern

208   since the late 1970s (Zhou 2009; Ding et al. 2009). The south flood-north drought pattern has

209   been predominantly attributed to internal variability, especially the phase change of the IPO (Li

210   et al. 2010, Nigam et al 2015, Ha et al. 2020a), and aided by GHG-induced warming (Zhu et al.

211   2012), and increased Asian aerosols emissions from the 1970s to 2000s (Dong et al., 2019).

212   Since 1979, both sea-surface temperature (SST) and atmospheric heating over Southeast Asia

213   and adjacent seas have increased significantly (Li et al. 2016), which may have led to decreased

214   rainfall over East Asia, South Asia (Annamalai et al., 2013) and the Sahel region (He et al. 2017).

215   Analysis of 16 CMIP6 models indicates that, under the SSP2-4.5 scenario, EASM

216   precipitation will increase at 4.7 %/°C (Ha et al. 2020b), with dynamic effects more important

217   than thermodynamic effects (Oh et al., 2018; Li et al. 2019). EASM duration is projected to

218   lengthen by about five pentads due to earlier onset and delayed retreat (Ha et al. 2020b), which

219   is comparable to previous assessment results (Endo et al. 2012, Kitoh et al. 2013, Moon and Ha

220   2017).

221   3.3 African monsoon

222   West Africa rainfall totals in the Sahel have been increasing since the 1980s, which

223   helped regreening (Taylor et al. 2017; Brandt et al. 2019). Much of the increase in seasonal

224   rainfall is owed to positive trends in mean intensity (Lodoun et al. 2013, Sarr et al. 2013),

225   rainfall extremes (Panthou et al. 2014, Sanogo et al. 2015), and the frequency of intense

226   mesoscale convective systems (Taylor et al. 2017). Several West African countries have

11

227 experienced trends towards a wetter late season and delayed cessation of the rains (Lodoun et

228 al. 2013, Brandt et al. 2019). All the above changes are qualitatively consistent with

229 the CMIP5 response to GHG (Marvel et al., 2019). Preliminary results from CMIP6

230 confirm that the Sahel will become wetter, except for the west coast, and the rainy season will

231 extend later (Supplementary Fig. S1). Yet, the range of simulated variability has not improved,

232 and large quantitative uncertainties in the projections persist. In spite of the large spread, the

233 CMIP6 models project that NAF land monsoon rainfall will likely increase (Fig. 3).

234   In East Africa, observed increases in the boreal fall short rains are more robust (e.g.,

235 Cattani et al. 2018) than negative trends in the spring long rains (e.g., Maidment et al. 2015).

236 Regionality is pronounced, and there is sensitivity to Indian Ocean SSTs and Pacific variability

237 (Liebmann et al. 2014; Omondi et al. 2013). Selected CMIP6 models project little agreement on

238 how East African rainfall will change (supplementary Fig. S2), while some regional models

239 suggest enhanced rainfall during the short rains and a curtailed long-rains season (Cook and

240 Vizy 2013; Han et al. 2019). In the Congo Basin, observed precipitation trends are inconclusive

241 (Zhou et al. 2014; Cook and Vizy 2019), but one study reports earlier onset of the spring rains

242 (Taylor et al. 2018). A preliminary analysis finds overall improvement in CMIP6 models in the

243 overestimation of Congo Basin rainfall, though projections of changes under the SSP2-4.5

244 scenario are inconsistent. (Supplementary Fig. S3).

245   The CMIP6 models project that under SSP2-4.5 scenario and by the latter part of 21st

246 century, the SAF land monsoon rainfall will likely increase in summer but considerably reduce in

247 winter, so that the annual range will amplify but the annual mean rainfall will not change

248 significantly (Fig. 3)

249   3.4 Australian monsoon

250   Observations show increasing trends in mean and extreme rainfall over northern,

251   especially northwestern Australia since the early 1970s (Dey et al. 2019). Although Australian

252   summer monsoon rainfall has exhibited strong decadal variations during the 20th and early 21st

253   century, making detection and attribution of trends challenging, the recent upward trend since

254   1970s has been attributed to direct thermal forcing by increasing SST in the tropical western

255   Pacific (Li et al. 2013) and to aerosol and GHG forcing (Rotstayn et al. 2007, Salzmann 2016).

256   Australian monsoon rainfall is projected to increase by an average of 0.4%/°C in 33

257   CMIP5 models (Dey et al. 2019), although there is a large spread in the magnitude and even the

258   direction of the projected change. By selecting the best performing models for the Australian

259   monsoon, Joudain et al. (2013) found that seven of ten "good" CMIP5 models indicate a 5-20%

260   increase in monsoon rainfall over northern (20°S) Australian land by the latter part of the

261   21st century, but trends over a much larger region of the Maritime Continent are more

262   uncertain. Narsey et al. (2019) found that the range in Australian monsoon projections from the

263   available CMIP6 ensemble is substantially reduced compared to CMIP5, however, models

264   continue to disagree on the magnitude and direction of change. The CMIP6 models project that

265   summer and annual mean LMR changes are insignificant under SSP2-4.5; but the winter LMR

266   will likely decrease (Fig. 3) due to the enhanced Asian summer monsoon. By the end of the 21st

267   century, the Madden-Julian Oscillation (MJO) is anticipated to have stronger amplitude rainfall

268   variability (Maloney et al. 2018), but the impact on Australian summer monsoon intraseasonal

269   variability is uncertain (Moise et al. 2019).

270   3.5 North American monsoon

271   Observed long-term 20th century rainfall trends are either negative or null, but the

272   trends can vary substantially within this region (Pascale et al., 2019). During the period of

273   1950-2010 the monsoonal ridge was strengthened and shifted the patterns of transient

274   inverted troughs making them less frequent in triggering severe weather (Lahmers et al., 2016).

275   Recent observational and modeling studies show an increase in the magnitude of extreme

276   events in NAM and Central American rainfall under anthropogenic global warming (Aguilar et

277   al., 2005; Luong et al., 2017).

278   Climate models suggest an early-to-late redistribution of the mean NAM precipitation

279   with no overall reduction (Seth 2013, Cook and Seager, 2013), and a more substantial reduction

280   for Central American precipitation (Colorado-Ruiz et al., 2019). However, there is low

281   confidence in these projections, since both local biases (the models' representation of

282   vegetation dynamics, land cover and use, soil moisture hydrology) and remote biases (current

283   and future SST) may lead to large uncertainties (Bukovsky et al., 2015; Pascale et al., 2017).

284   Confidence in mean precipitation changes is lower than in the projection that precipitation

285   extremes are likely to increase due to the changing thermodynamic environment (Luong et al.

286   2017; Prein et al., 2016).

287   Figure 5 schematically sums up the factors that are likely to be determinant in the future

288   behavior of the NAM: the expansion and northwestward shift of the NAM ridge, and the

289   strengthening of the remote stabilizing effect due to SST warming are shown, and more intense

290   MCS-type convection. More uncertain remains the future of the NAM moisture surges and the

291   track of the upper-level inverted troughs, which are key synoptic processes controlling

292   convective activity.

293   3.6 South American monsoon

294   A significant positive precipitation trend since the 1950s till the 1990s was observed in

295   southeast South America, and has been related to interdecadal variability (Grimm and Saboia,

296   2015), ozone depletion and increasing GHG (Gonzalez et al. 2014; Vera and Diaz 2015). The

297   trend in the tropical South American monsoon is less coherent due to the influence of the

298   tropical Atlantic and the tendency to reverse rainfall anomalies from spring to summer in the

299   central-east South America due to land-atmosphere interactions (Grimm et al. 2007). In recent

300   decades the dry season has been lengthened and become drier, especially over the southern

301   Amazonia, which has significant influences on vegetation and moisture transport to the SAM

302   core region (Fu et al. 2013).

303   The CMIP6 models-projected future precipitation changes resemble the anomalies

304   expected for El Niño: little change of total precipitation (Figs. 3 and 4). This is consistent with El

305   Niño impacts (Grimm 2011) and CMIP5 projections (Seth et al. 2013). CMIP5 also projected

306   reduction of early monsoon rainfall while peak season rainfall increases, a delay and shortening

307   of the monsoon season (Seth et al. 2013), and prolonged dry spells between the rainy events

308   (Christensen et al., 2013). However, inter-model discrepancies are large (Yin et al., 2013).

309   CMIP5 models also likely underestimate the climate variability of the South American monsoon

310   and its sensitivity to climate forcing (Fu et al., 2013). Bias-corrected projections generally show

311   a drier climate over eastern Amazonia (e.g., Duffy et al., 2015; Malhi et al., 2008). Thus, the risk

312   of strong climatic drying and potential rainforest die-back in the future remains real.

313   **4. Extreme precipitation events in summer monsoons**

314   4. 1. Past changes and attribution

15

Over the past century, significant increases in extreme precipitation in association with global warming have emerged over the global land monsoon region as a whole, and annual maximum daily rainfall has increased at the rate of about 10-14%/°C in the southern part of the South African monsoon, about 8%/°C in the South Asian monsoon, 6-11%/°C in the NAM, and 15-25%/°C in the eastern part of the South American monsoon (Zhang and Zhou 2019). At Seoul, Korea, one of the world's longest instrumental measurements of daily precipitation since 1778 shows that the annual maximum daily rainfall and the number of extremely wet days, defined as the 99th percentile of daily precipitation distribution, all have an increasing trend significant at the 99% confidence level (Fig. 6). In the central Indian subcontinent, a significant shift towards heavier precipitation in shorter duration spells occurred from 1950–2015 (Fig. 7) (Roxy et al. 2017, Singh et al. 2019). In East Asia, the average extreme rainfall trend increased from 1958 to 2010, with a decreasing trend in northern China that was offset by a much larger increasing trend in southern China (Chang et al. 2012). Over tropical South America, extreme indices such as annual total precipitation above the 99th percentile and the maximum number of consecutive dry days display more significant and extensive trends (Skansi et al. 2013, Hilker et al. 2014).

Attribution studies show that global warming has already increased the frequency of heavy precipitation since the mid-20th Century. An optimal fingerprinting analysis shows that anthropogenic forcing has made a detectable contribution to the observed shift towards heavy precipitation in eastern China (Ma et al. 2017). Simulations with all and natural-only forcing show that global warming increased the probability of the 2016 Yangtze River extreme summer rainfall by 17%–59% (Yuan et al. 2018). A large ensemble experiment also showed that

16

337   historical global warming has increased July maximum daily precipitation in western Japan

338   (Kawase et al. 2019).

339   Another anthropogenic forcing is urbanization. A significant correlation between rapid

340   urbanization and increased extreme hourly rainfall has been detected in the Pearl River Delta

341   and Yangtze River Delta of coastal China (Fig. 8) (Wu et al. 2019, Jiang et al. 2019). The

342   increasing trends are larger in both extreme hourly rainfall and surface temperature at urban

343   stations than those at nearby rural stations. The correlation of urbanization and extreme

344   rainfall is due to the urban heat island effect, which increases instability and facilitates deep

345   convection. Large spatial variability in the trends of extreme rainfall in India due to urbanization

346   and changes in land-use and land-cover has also been detected (Ali and Mishra 2017).

347   Land-falling tropical cyclones (TCs) make large contributions to heavy precipitation in

348   coastal East Asia. In the last 50 years, the decreasing frequency of incoming western North

349   Pacific (WNP) TCs more than offsets the increasing TC rainfall intensity, resulting in reduced TC-

350   induced extreme rainfall in southern coastal China, so the actual increase in non-TC extreme

351   rainfall is even larger than observed (Chang et al. 2012). Evidence in the WNP, and declining TC

352   landfall in eastern Australia (Nicholls et al. 1998), suggest that this poleward movement reflects

353   greater poleward TC recurvature.

354   4.2. Future Projection

355   One of the most robust signals of projected future change is the increased occurrence of

356   heavy rainfall on daily-to-multiday time scales and intense rainfall on hourly time scales. Heavy

357   rainfall will increase at a much larger rate than the mean precipitation, especially in Asia (Kitoh,

358   2013, 2017). Unlike mean precipitation changes, heavy and intense rainfall is more tightly

17

359 controlled by the environmental moisture content related to the Clausius-Clapeyron

360 relationship and convective-scale circulation changes. On average, extreme five-day GM rainfall

361 responds approximately linearly to global temperature increase at a rate of 5.17 (4.14–

362 5.75)%/°C under RCP8.5 with a high signal-to-noise ratio (Zhang et al. 2018). Regionally,

363 extreme precipitation in the Asian monsoon region exhibits the highest sensitivity to warming,

364 while changes in the North American and Australian monsoon regions are moderate with low

365 signal-to-noise ratio (Zhang et al. 2018). CMIP6 models project changes of extreme 1-day

366 rainfall of +58% over South Asia and +68% over East Asia in 2065–2100 compared to 1979–2014

367 under the SSP2-4.5 scenario (Ha et al. 2020b). Model experiments also indicate a three-fold

368 increase in the frequency of rainfall extremes over the Indian subcontinent under future

369 projections for global warming of 1.5°C–2.5°C (Bhowmick et al. 2019). Meanwhile, light-to-

370 moderate rain events may become less frequent (Sooraj et al. 2016).

371 Changes in the variability of monsoon rainfall may occur on a range of time scales.

372 Brown et al. (2017) found increased rainfall variability under RCP8.5 for each time scale from

373 daily to decadal over the Australian, South Asian, and East Asian monsoon domains (Fig. 8). The

374 largest fractional increases in monsoon rainfall variability occur for South Asian at all sub-

375 annual time scales and for the East Asian monsoon at annual-to-decadal time scales. Future

376 changes in rainfall variability are significantly positively correlated with changes in mean wet

377 season rainfall for each of the monsoon domains and for most time scales.

378 Selected CMIP5 models project more severe floods and droughts in the future climate

379 over South Asia (Sharmila et al. 2015; Singh et al. 2019). Due to more rapidly rising evaporation,

380 the projections for 2015–2100 under CMIP6 SSP2-4.5 and SSP5-8.5 scenarios indicate that the

18

381   western part of East Asia will confront more rapidly increasing drought severity and risks than

382   the eastern part (Ha et al. 2020b).

383   Projections of future extreme rainfall change in the densely populated and fast-growing

384   coastal zones are particularly important for several reasons. First, in fast-growing urban areas,

385   extreme rainfall will likely intensify in the future, depending on the economic growth of the

386   affected areas. Second, future extreme rainfall changes in coastal areas will be affected by

387   future changes in landfalling TCs. For instance, TC projections (Knutson et al. 2019b) suggest a

388   continued (albeit with lower confidence) northward trend. Assuming this means more

389   recurvature cases, it would lead to extreme rainfall increases in coastal regions of Korea and

390   Japan and decreases in China. Third, the increase in monsoon extreme rains and TCs, together

391   with rising sea level will lead to aggravated impacts, for instance, along coastal regions of the

392   Indian subcontinent (Collins et al. 2019).

393   **5. Model Issues and Future Outlook**

394   5.1 Major common issues and missing processes

395   CMIP6 models improve the simulation of present-day solstice season precipitation

396   climatology and the GM precipitation domain and intensity over the CMIP5 models; and CMIP6

397   models reproduce well the annual cycle of the NH monsoon and the leading mode of GM

398   interannual variability and its relationship with ENSO (Wang et al. 2020). However, the models

399   have major common biases in equatorial oceanic rainfall and SH monsoon rainfall, including

400   overproduction of annual mean SH monsoon precipitation by more than 20%, and the

401   simulated onset is early by two pentads while the withdrawal is late by 4-5 pentads (Wang et al.

402   2020). Systematic model biases in monsoon climates have persisted through generations of

403   CMIP (e.g., Sperber et al., 2013). In particular, the poor representation of precipitation

404   climatology is seen in many regional monsoons, such as Africa (Creese and Washington 2016,

405   Han et al. 2019), and North America (Geil et al., 2013). These biases are often related to SST

406   biases in adjacent oceans (Cook and Vizy 2013, Pascale et al., 2017). There are additional

407   outstanding common issues for regional monsoon simulations, which are not immediately

408   apparent in quick-look analyses. A major one is the diurnal cycle, which is poorly simulated in

409   the tropics, due to failures in convective parameterization (Willetts et al., 2017). Biases in

410   evapotranspiration also affect the Bowen ratio (Yin et al. 2013), and thus atmospheric boundary

411   layer humidity and height. Biases in variability emerge in historical monsoon simulations,

412   hampering accurate attribution of present-day monsoon changes (Herman et al. 2019; Marvel

413   et al, 2019) and amplifying uncertainties in future projections.

414   While there are subtle improvements from CMIP3 to CMIP5 and to CMIP6 due to steady

415   increases in horizontal resolution and improved parameterizations, simulation of monsoon

416   rainfall is still hampered by missing or poorly resolved processes. These include the lack of

417   organized convection (e.g., mesoscale convective systems or monsoon depressions) at coarse

418   model resolutions, poorly simulated orographic processes, and imperfect land-atmosphere

419   coupling due to under-developed parametrizations and a paucity of observations of land-

420   atmosphere exchanges that can only be improved through field observation programs (e.g.

421   Turner et al., 2019). Further, proper simulation of how aerosols modify monsoon rainfall

422   requires improved cloud microphysics schemes (Yang et al., 2017; Chu et al., 2018). Finally,

423   some features of monsoon meteorology that are crucial to climate projection and adaptation,

424   such as extreme rainfall accumulations exceeding 1 meter/day, are nearly impossible to

425   simulate in coupled climate models. High-resolution regional simulations can potentially

426   ameliorate biases, but they still must rely on GCM-generated boundary conditions in their

427   projections. Convection-permitting regional simulations have been suggested to more

428   realistically represent short time scale rainfall processes and their responses to forcing (e.g. in

429   future simulations for Africa; Kendon et al., 2019).

430   5.2 Sources of model uncertainty in future projection of monsoons

431   The major sources of projection uncertainty include model uncertainty, scenario

432   uncertainty and internal variability. Contributions from internal variability decrease with time,

433   while those from scenario uncertainty increase. Model uncertainty dominates near-term

434   projections of GM mean and extreme precipitation with a contribution of ~90% (Zhou et al.

435   2020a). Model uncertainty often arises from divergent circulation changes. In particular,

436   circulation changes caused by regional SST warming and land-sea thermal contrast can

437   generally contribute to uncertainty in monsoon rainfall changes (Chen and Zhou, 2015; Pascale

438   et al., 2017). Uncertainty in projected surface warming patterns is closely related to present-

439   day model biases, including the cold-tongue bias in the tropical eastern Pacific (Chen and Zhou,

440   2015; Ying et al. 2019) and a cold bias beneath underestimated marine stratocumulus, which

441   can induce a large land-sea thermal contrast in the future (Nam et al. 2012, Chen et al. 2019).

442   Monsoons are strongly influenced by cloud and water vapor feedbacks (Jalihal et al., 2019;

443   Byrne and Zanna, 2020), yet how the large variations in these feedbacks across climate models

444   impact monsoon uncertainties is unknown. Another factor affecting future monsoon changes

445   are vegetation feedbacks. Cui et al. (2019) showed that they may exacerbate the effects of CO_2-

446   induced radiative forcing, especially in the North and South American and Australian monsoons

447   via reduced stomatal conductance and transpiration. Vegetation is an important water vapor

448   provider and can affect monsoon onsets (Wright et al. 2017; Sori et al. 2017), yet current

449   climate models have limited capability in representing how vegetation responds to climate and

450   elevated CO_2, and how land use and fires affect future vegetation distribution and functions.

451   The extent to which these model limitations contribute to the uncertainty of future monsoon

452   rainfall projections is virtually unknown, although plant physiological effects may exacerbate

453   CO_2-raditiative impacts (Cui et al., 2019). While CMIP6 models are more advanced in terms of

454   physical processes included and resolution, the inter-model spread in projection of monsoons

455   in CMIP6 models has remained as large (or became larger) compared to CMIP5 models (Fig 2).

456   5.3 Future Outlook

457   Future models might improve by explicitly resolving deep convection to address

458   common problems across monsoon systems. In attribution, controversies remain over the

459   relative roles of natural multidecadal variability and anthropogenic forcing, especially of aerosol

460   effects on the observed historical monsoon evolution in Asia and West Africa. Quantification of

461   the roles of multidecadal variability in biasing the transient climate sensitivity in observations as

462   well as in model simulations is encouraged.

463   There is an urgent need to better understand sources of uncertainty in future rainfall

464   projections. Such sources encompass but are not limited to structural uncertainty, uncertainties

465   in aerosol processes and radiative forcing, the roles of internal modes of variability and their

466   potential changes in the future, ecosystem feedbacks to climate change and elevated CO_2, and

467   land-use impacts. To have more confidence in future projections, we need to quantify the

468   causes of spread in future climate signals at the process level: the relative magnitudes of

469 forcing uncertainty versus mean-state biases and feedback uncertainties. This type of error

470 quantification requires specially designed, coordinated simulations across modelling centers

471 and a focus on the key processes that need to be improved.

472   Traditional future assessments of the global monsoon continue to rely on multi-model

473 approaches. However, a small multi-model ensemble such as CMIP5 or CMIP6 may not

474 represent the full extent of uncertainty introduced by internal (multi-decadal) variability. More

475 recently, large ensembles are being employed to help understand the spread or degree of

476 uncertainty in a climate signal, and, at the regional level, the interplay between internal

477 variability and anthropogenic external forcing in determining a climate anomaly. Such large

478 ensembles are either perturbed-parameter ensembles (PPE) (Murphy et al., 2014) or

479 alternatively, traditional initial-condition ensembles – e.g., by CanESM2 (Sigmond and Fyfe,

480 2016; Kirchmeier-Young, 2017) or by MPI-ESM (Maher et al., 2019) – with tens to a hundred

481 members. Large-ensemble methods should be applied to the global monsoon in order to

482 determine the extent to which internal variability can explain its declining rainfall in the late

483 20th century. We suggest that an additional pathway to more reliable monsoon projections

484 would be to develop emergent constraints applicable to monsoons, and this should be a focus

485 for the research community.

486   Recent theoretical advances in tropical atmospheric dynamics offer new avenues to

487 further our understanding of monsoon circulations in a changing climate. Monsoon locations

488 have been shown to coincide with maxima in sub-cloud moist static energy (MSE) (Privé and

489 Plumb 2007), with MSE budgets likely to be useful for understanding the response of monsoons

490 to external forcing (Hill 2019). Recent studies of the ITCZ may also provide new insights into the

23

491   strength and spatial extent of monsoons. Theoretical work has identified energetic (Sobel and

492   Neelin, 2006; Byrne and Schneider, 2016) and dynamical constraints (Byrne and Thomas, 2019)

493   on the width of the ITCZ, with implications for its strength (Byrne et al., 2018). Additionally,

494   Singh et al. (2017) have linked the strength of the Hadley circulation to meridional gradients in

495   moist entropy. The extent to which these theories can explain CMIP6 changes in monsoon

496   strength and spatial extent is an open question that should be prioritized.

497   Understanding past monsoon responses to external forcings may shed light on future

498   climate change. The NH monsoon future response is shown to be weaker than in simulations of

499   the mid-Holocene, although future warming is larger (D'Agostino et al. 2019). This occurs

500   because both thermodynamic and dynamic responses act in concert and cross-equatorial

501   energy fluxes shift the ITCZ towards the warmer NH during the mid-Holocene, but in the future,

502   they partially cancel. The centennial-millennial variations of GM precipitation before the

503   industrial period are mainly attributable to solar and volcanic (SV) forcing (Liu et al., 2009). For

504   the same degree of warming, GHG forcing induces less rainfall increase than SV forcing because

505   the former increases stability, favoring a weakened Walker circulation and El Niño-like warming,

506   while the latter warms tropical Pacific SSTs in the west more than the east, favoring a La Nina-

507   like warming through the ocean thermostat mechanism (Liu et al. 2013). An El Niño-like

508   warming reduces GM precipitation (Wang et al. 2012). Jalihal et al. (2019), by examining

509   responses of tropical precipitation to orbital forcing, find that the changes in precipitation over

510   land are mainly driven by changes in insolation, but over the oceans, surface fluxes and vertical

511   stability play an important role in precipitation changes.

512   **6. Summary**

513   We have reviewed past monsoon changes and their primary drivers, summarized

514   projected future changes and key physical processes, and discussed challenges of the present

515   and future modeling and outlooks. In this section we will assign a level of confidence to the

516   main conclusions wherever feasible.

517   *1. Extreme rainfall events.*

518   Continued global warming over the past century has already caused a significant rise in

519   the intensity and frequency of extreme rainfall events in all monsoon regions (e.g., Figs. 6 and 7;

520   high confidence). Urbanization presents additional anthropogenic forcing that significantly

521   increases localized extreme rainfall events in areas of rapid economic growth due to the urban

522   heat island effect (Fig. 8, high confidence). This urban effect is expected to expand to more

523   locations with the growing economy, especially in Asia. There is some indication that TC tracks

524   in the western North Pacific have been shifting more towards the recurvature type. If this trend

525   continues, it may cause an increase in the ratio of TC-related extreme rainfall in Korea and

526   Japan versus China (low confidence).

527   Almost all future projections agree that the frequency and intensity of extreme rainfall

528   events will increase. The occurrence of heavy rainfall will increase on daily-to-multiday time

529   scale and intense rainfall on hourly time scales. The increased extreme rainfall is largely due to

530   an increase in available moisture supply and convective-scale circulation changes. Meanwhile,

531   models also project prolonged dry spells between the heavy rainy events, which, along with

532   enhanced evaporation and runoff of ground water during heavy rainfall, will lead to an

533   increased risk of droughts over many monsoon regions (high confidence). Notably, the

25

534   enhanced extreme rain events will *likely* contribute to compound events—where increasing

535   tropical cyclones, rising sea level, and changing land conditions—may aggravate the impact of

536   floods over the heavily populated coastal regions.

537   *2. Mean monsoon rainfall and its variability*

538   Observed changes in the mean monsoon rainfall vary by region with significant decadal

539   variations that have been related to internal modes of natural variability. Since the 1950s, NH

540   anthropogenic aerosols may be a significant driver in the Sahel drought and decline of monsoon

541   rainfall in South Asia (medium-high confidence). NH land monsoon rainfall as a whole declined

542   from 1950 to 1980 and rebounded after the 1980s, due to the competing influence of internal

543   climate variability, radiative forcing from GHGs and aerosol forcing (high confidence); however,

544   it remains a challenge to quantify their relative contributions. CMIP6 historical simulations

545   suggest that anthropogenic sulfate and volcanic forcing likely masked the effect of GHG forcing

546   and caused the downward trend from 1950 to 1990 (Fig. 2); however, the recent upward trend

547   may signify the emergence of the greenhouse-gas signal against the rainfall reduction due to

548   aerosol emissions (medium-high confidence).

549   CMIP6 models project a larger increase in monsoon rainfall over land than over ocean

550   (Fig. 2). Land monsoon rainfall will likely increase in the NH, but change little in the SH (Figs. 2

551   and 4). Regionally, land monsoon rainfall will increase in South Asia and East Asia (high

552   confidence), and northern Africa (medium confidence), but decrease over North American

553   monsoon region (high confidence) (Fig. 3). The projected mean rainfall changes (either neutral

554   or slightly decreasing) over SH (American, Australian, and Southern African) monsoons have low

26

555   confidence due to a large spread. The future change of GM precipitation pattern and intensity

556   is determined by increased specific humidity and circulation changes forced by the vertically

557   and horizontally inhomogeneous heating induced by GHG radiative forcing. Under GHGs-

558   induced warming, the land monsoon rainy season changes considerably from region to region;

559   yet, as a whole, the rainy season will likely be lengthened in the NH due to late retreat (with

560   most significant change over East Asia), but shortened in the SH due to delayed onset. The

561   variability of monsoon rainfall is projected to increase on daily to decadal time scales over the

562   Asian-Australian monsoon region (Fig. 9). Models generally underestimate the magnitude of

563   observed precipitation changes, which poses a major challenge for quantitative attributions of

564   regional monsoon changes. The range of projected change of annual-mean global land

565   monsoon precipitation by the end of the 21st century in CMIP6 is *likely* about 50% larger than in

566   corresponding scenarios of CMIP5.

567

589   **References**

590   Abbs, D., 2012: The impact of climate change on the climatology of tropical cyclones in the

591   Australian region. *Aspendale: CSIRO,* **11,** doi:10.4225/08/584ee7d4585f5.

592   Aguilar, E., T. C. Peterson, P. Ramírez Obando, R. Frutos, J. A. Retana, M. Solera, J. Soley, I.

593   González García, R. M. Araujo, A. Rosa Santos, V. E. Valle, M. Brunet, L. Aguilar, L.

594   Álvarez, M. Bautista, C. Castañón, L. Herrera, E. Ruano, J. J. Sinay, E. Sánchez, G. I.

595   Hernández Oviedo, F. Obed, J. E. Salgado, J. L. Vázquez, M. Baca, M. Gutiérrez, C.

596   Centella, J. Espinosa, D. Martínez, B. Olmedo, C. E. Ojeda Espinoza, R. Núñez, M.

597   Haylock, H. Benavides, and R. Mayorga 2005: Changes in precipitation and temperature

598   extremes in Central America and northern South America, 1961–2003. *J. Geophys. Res.,*

599   **110,** D23107.

600   Ali, H., and V. Mishra, 2017: Contrasting response of rainfall extremes to increase in surface air

601   and dewpoint temperatures at urban locations in India. Scientific Reports, 7, 1228.

602   Annamalai, H., J. Hafner, K. P. Sooraj and P. Pillai, 2013: Global warming shifts the monsoon

603   circulation, drying South Asia. J. Climate, 26, 2701-2718.

604   Bayr, T., D. Dommenget, T. Martin, and S. B. Power, 2014: The eastward shift of the Walker

605   circulation in response to global warming and its relationship to ENSO variability.

606   *Climate Dyn.,* **43,** 2747–2763, doi:10.1007/s00382-014-2091-y.

607   Bhowmick, M., S. Sahany, and S. K. Mishra, 2019: Projected precipitation changes over the

608   south Asian region for every 0.5° C increase in global warming. *Environ. Res. Lett.,* **14,**

609   054005, doi:10.1088/1748-9326/ab1271.

610   Bollasina, M. A., Y. Ming, and V. Ramaswamy, 2011: Anthropogenic aerosols and the weakening

611   of the South Asian summer monsoon. *Science,* **334,** 502-505.

612   Byrne, M. P., and T. Schneider, 2016: Narrowing of the ITCZ in a warming climate: physical

613   mechanisms. *Geophys. Res. Lett.,* **43,** 350.

614   Byrne, M. P., A. G. Pendergrass, A. D. Rapp, and K. R. Wodzicki, 2018: Response of the

615   intertropical convergence zone to climate change: Location, width, and strength.

616   *Current Climate Change Reports,* **4,** 355–370, doi:10.1007/s40641-018-0110-5.

617   Byrne, M. P., and R. Thomas, 2019: Dynamics of ITCZ width: Ekman processes, non-Ekman

618   processes, and links to sea surface temperature. *J. Atmos. Sci.,* **76,** 2869–2884.

619   Byrne, M. P., and L. Zanna, 2020: Radiative effects of clouds and water vapor on the monsoon.

620   *J. Climate*, in revision (preprint available at

621   https://drive.google.com/file/d/1HJgsclJlqFR_tFFVHB-NxoyzJdQjJk4J/view).

622   Bukovsky, M. S., C. M. Carrillo, D. J. Gochis, D. M. Hammerling, R. R. McCrary, and L. O. Mearns,

623   2015: Toward assessing NARCCAP Regional Climate Model credibility for the North

624   American Monsoon: future climate simulations. *J. Climate,* **28,** 6707–6728.

625   Cai, W., X.-T. Zheng, E. Weller, M. Collins, T. Cowan, M. Lengaigne, T. Yamagata, 2013: Projected

626   response of the Indian Ocean dipole to greenhouse warming. *Nature Geoscience,* **6,**

627   999–1007.

628   Cai, W., G. Wang, A. Santoso, M. J. McPhaden, L. Wu, F.-F. Jin, and E. Guilyardi, 2015: Increased

629   frequency of extreme La Niña events under greenhouse warming. *Nature Climate*

630   *Change,* **5,** 132–137.

631   Cattani, E., A. Merino, J. A. Guijarro, and V. Levizzani, 2018: East Africa rainfall trends and

632   variability 1983–2015 using three long-term satellite products. *Remote Sensing,* **10,** 931,

633   doi:10.3390/rs10060931.

634   Chang, C. W. J., W.-L. Tseng, H.-H. Hsu, N. Keenlyside, and B.-J. Tsuang, 2015: The Madden-

635   Julian oscillation in a warmer world. *Geophy. Res. Lett.*, *42,* 6034–6042.

636   Chang, C.-P., M. Ghil, H.C. Kuo, M. Latif, C. H. Sui, and J. M. Wallace, 2014: Understanding

637   multidecadal climate changes. *Bull. Am. Meteorol. Soc.,* **95**, 293–296. doi:

638   10.1175/BAMS-D-13-00015.1.

639   Chang, C.-P., Y. Lei, C.-H. Sui, X. Lin, and F. Ren, 2012: Tropical cyclone and extreme rainfall

640   trends in East Asian summer monsoon since mid-20th century, Geophys. Res. Lett., 39,

641   L18702, doi:10.1029/2012GL052945.

642   Chang, C.-P., Z. Wang, J. McBride and C. H. Liu, 2005: Annual cycle of Southeast Asia - Maritime

643   Continent rainfall and the asymmetric monsoon transition. *J. Climate,* **18**, 287-301.

644   Chen, X., and T. Zhou, 2015: Distinct effects of global mean warming and regional sea surface

645   warming pattern on projected uncertainty in the South Asian summer monsoon.

646   *Geophys. Res. Lett.,* **42,** 9433–9439.

647   Chen, X., T. Zhou, P. Wu, Z. Guo, and M. Wang, 2019: Emergent constraints on future

648   projections of the western North Pacific Subtropical High. *Nat. Commun.,* under review.

649   Manuscript is available at https://drive.google.com/open?id=1hkuL4G_xQ-

650   2B6PBYGSMHXDhBrcAARaPZ

651   Christensen, J.H., K. Krishna Kumar, E. Aldrian, S.-I. An, I.F.A. Cavalcanti, M. de Castro, W. Dong,

652   P. Goswami, A. Hall, J.K. Kanyanga, A. Kitoh, J. Kossin, N.-C. Lau, J. Renwick, D.B.

653   Stephenson, S.-P. Xie and T. Zhou, 2013: Climate Phenomena and their Relevance for

654   Future Regional Climate Change. In: Climate Change 2013: The Physical Science Basis.

655   Contribution of Working Group I to the Fifth Assessment Report of the

656   Intergovernmental Panel on Climate Change [Stocker, T.F., D. Qin, G.-K. Plattner, M.

657   Tignor, S.K. Allen, J. Boschung, A. Nauels, Y. Xia, V. Bex and P.M. Midgley (eds.)].

658   Cambridge University Press, Cambridge, United Kingdom and New York, NY, USA.

659 Chu, J.-E., K.-M. Kim, W. K. M. Lau and K.-J. Ha, 2018: How light absorbing properties of organic

660   aerosol modify the Asian summer monsoon rainfall? *J. Geophys. Res. Atmos.,* **123,** 2244–

661   2255, doi:10.1002/2017JD027642.

662 Collins, M., and Coauthors, 2019: Extremes, Abrupt Changes and Managing Risk, in Portner et

663   al., eds. IPCC Special Report on Oceans and Cryosphere in a Changing Climate.

664   Cambridge University Press, Cambridge, United Kingdom and New York, NY, USA.

665 Cook, B. I. and R. Seager, 2013: The response of the North American Monsoon to increased

666   greenhouse gas forcing. *J. Geophys. Res.,* **118,** 1690–1699.

667 Cook, K. H., and E. K. Vizy, 2013: Projected changes in East African rainy seasons. *J. Climate,* **26,**

668   5931–5948, doi:10.1175/JCLI-D-12-00455.1

669 Cook, K. H., and E. K. Vizy, 2019: Congo Basin drying associated with poleward shifts of African

670   thermal lows. *Climate Dyn.,* doi:10.1007/s00382-019-05033-3.

671 Creese, A., and R. Washington, 2016: Using qflux to constrain modeled Congo Basin rainfall in

672   the CMIP5 ensemble. *J. Geophys. Res.,* **121,** 13415–13442, doi:10.1002/2016JD025596.

673 Cui, J., S. Piao, C. Huntingford, X. Wang, X. Lian, A. Chevuturi, A. G. Turner and G. J. Kooperman,

674   2019: Vegetation forcing modulates global land monsoon and water resources in a CO2-

675   enriched climate. Nature Geosciences, submitted. The latest version of this paper is

676   available   at: https://livereadingac-

677   my.sharepoint.com/:f:/g/personal/a_g_turner_reading_ac_uk/

678   El8hjGgHjs5KooEbLEP0lIIBGgSajLIwumjN9ARCV7lJNQ?e=GrH4NI

679 D'Agostino, R., J. Bader, S. Bordoni, D. Ferreira, and J. Jungclaus, 2019: Northern Hemisphere

680   monsoon response to mid-Holocene orbital forcing and greenhouse gas-induced global

681   warming. *Geophys. Res. Letts.,* **46,** 1591–1601, doi:10.1029/2018GL081589.

682 Deser, C., A. S. Phillips, and M. A. Alexander, 2010: Twentieth century tropical sea surface

683   temperature trends revisited. *Geophys. Res. Lett.,* **37,** L10701.

684 Dey, R., S. C. Lewis, J. M. Arblaster, and N. J. Abram, 2019: A review of past and projected

685   changes in Australia's rainfall. *Wiley Interdiscip. Rev. Clim. Chang.,* **10,** 1–23,

686   doi:10.1002/wcc.577.

687 Ding, Y., Y. Sun, Z. Wang, Y. Zhu, and Y. Song, 2009: Inter-decadal variation of the summer

688   precipitation in China and its association with decreasing Asian summer monsoon Part

689   II: Possible causes, Int. J. Climatology, 29, 1926-1944.

690 Dong, B., L. J. Wilcox, E. J. Highwood, and R. T. Sutton, 2019: Impacts of recent decadal changes

691   in Asian aerosols on the East Asian summer monsoon: roles of aerosol–radiation and

692   aerosol–cloud interactions. *Climate Dyn.,* **53,** 3235, doi:10.1007/s00382-019-04698-0.

693 Duffy, P. B., P. Brando, G. P. Asner, and C. B. Field, 2015: Projections of future meteorological

694   drought and wet periods in the Amazon. *Proc. Natl. Acad. Sci. USA,* **112,** 13172–13177,

695   doi:10.1073/pnas.1421010112.

696 Endo, H., A. Kitoh, T. Ose, R. Mizuta, and S. Kusunoki, 2012: Future changes and uncertainties in

697   Asian precipitation simulated by multiphysics and multi–sea surface temperature

698   ensemble experiments with high-resolution Meteorological Research Institute

699   atmospheric general circulation models (MRI-AGCMs). *J. Geophys. Res.,* **117,** D16118,

700   doi:10.1029/2012JD017874.

701 Endo, H., and A. Kitoh, 2014: Thermodynamic and dynamic effects on regional monsoon rainfall

702   changes in a warmer climate. *Geophys. Res. Lett.,* **41,** 1704–1711.

703 Endo, H., A. Kitoh, and H. Ueda, 2018: A unique feature of the Asian summer monsoon

704   response to global warming: the role of different land–sea thermal contrast change

705   between the lower and upper troposphere. *SOLA*, **14,** 57–63, doi:10.2151/sola.2018-

706   010.

707 Fu, R., L. Yin, W. Li, P. A. Arias, R. E. Dickinson, L. Huang, S. Chakraborty, K. Fernandes, B.

708   Liebmann, R. Fisher, and R. B. Myneni, 2013: Increased dry-season length over southern

709   Amazonia in recent decades and its implication for future climate projection. *Proc. Natl.*

710   *Acad. Sci. USA,* **110,** 18110–18115, doi:10.1073/pnas.1302584110.

711 Geil, K. L., Y. L. Serra, and X. Zeng, 2013: Assessment of CMIP5 Model Simulations of the North

712   American Monsoon System. *J. Climate,* **26,** 8787–8801, doi:10.1175/JCLI-D-13-00044.1.

713 Giannini, A, and A. Kaplan, 2019: The role of aerosols and greenhouse gases in Sahel drought

714   and recovery. *Climatic Change*, 152, 449-466.

715 Gonzalez, P. L. M., L. M. Polvani, R. Seager, G. J. Correa, 2014: Stratospheric ozone depletion: a

716   key driver of recent precipitation trends in South Eastern South America. *Climate Dyn.,*

717   **42,** 1775–1792.

718   Goswami, B. N., V. Venugopal, D. Sengupta, M. Madhusoodanan, and P. K. Xavier, 2006:

719   Increasing trend of extreme rain events over India in a warming environment. *Science,*

720   **314,** 1442–1445.

721   Grimm, A. M., J. Pal, and F. Giorgi, 2007: Connection between spring conditions and peak

722   summer monsoon rainfall in South America: Role of soil moisture, surface temperature,

723   and topography in eastern Brazil. *J. Climate,* **20,** 5929-5945.

724   Grimm, A. M., 2011: Interannual climate variability in South America: impacts on seasonal

725   precipitation, extreme events and possible effects of climate change. *Stochastic*

726   *Environmental Research and Risk Assessment*, 25, 537-554, DOI: 10.1007/s00477-010-

727   0420-1

728   Grimm, A. M., and J. P. J. Saboia, 2015: Interdecadal variability of the South American

729   precipitation in the monsoon season. *J. Climate,* **28,** 755-775, doi:10.1175/JCLI-D-14-

730   00046.1.

731   Ha, K. J., B. H. Kim, E. S. Chung, J. C. L. Chan, and C. P. Chang, 2020a: Major factors of monsoon

732   rainfall changes:natural versus anthropogenic forcing. *Environ. Res. Lett.,* doi:10.1088

733   /1748-9326/ab7767.

734   Ha, K. J., S. Moon, D. Kim, A. Timmermann, and D. Kim, 2020b: Future changes of summer

735   monsoon characteristics and evaporative demand over Asia in CMIP6 simulations.

736   Geophys. Res. Lett., doi:10.1029/2020GL087492.

737   Han, F., K. H. Cook, E. K. Vizy, 2019: Changes in intense rainfall events and drought across Africa

738   in the 21st century. *Climate Dyn.,* 53, 2757-2777. doi:10.1007/s00382-019-04653-z.

739   He, B., S. Yang, and Z. Li, 2016: Role of atmospheric heating over the South China Sea and

740   western Pacific regions in modulating Asian summer climate under the global warming

741   background. Climate Dyn., 46, 2897-2908.

742   He, S., S. Yang, and Z. Li, 2017: Influence of latent heating over the Asian and western Pacific

743   monsoon region on Sahel summer rainfall. Sci. Reports, 7, 7680,

744   https://doi.org/10.1038/s41598-017-07971.

745   Held, I. M. and B. J. Soden, 2006: Robust responses of the hydrological cycle to global warming.

746   *J. Climate,* **19,** 5686–5699.

747   Herman, R. J., A. Giannini, M. Biasutti, and Y. Kushnir, 2019: The Effects of Anthropogenic and

748   Volcanic Aerosols and Greenhouse Gases on 20th Century Sahel Precipitation. *Scientific*

749   *Reports,* submitted*.*

750   Hilker, T., A. I. Lyapustin, C. J. Tucker, F. G. Hall, R. B. Myneni, Y. Wang, J. Bi, Y. M. de Moura,

751   and P. J. Sellers, 2014: Vegetation dynamics and rainfall sensitivity of the Amazon. *Proc.*

752   *Natl. Acad. Sci. USA,* **111,** 16041–16046, doi:10.1073/pnas.1404870111

753   Hill, S. A., 2019: Theories for Past and Future Monsoon Rainfall Changes. *Current Climate*

754   *Change Reports,* **5,** 160-171.

755   Hsu, P.-C., T. Li, H. Murakami and A. Kitoh, 2013: Future change of the global monsoon revealed

756   from 19 CMIP5 models. *J. Geophys. Res. Atmos.,* **118,** 1247–1260.

757   Huang, P., S.-P. Xie, K. Hu, G.Huang and R. Huang, 2013: Patterns of the seasonal response of

758   tropical rainfall to global warming, Nature Geos., 6, 357-361.

759   Huang, X., T. Zhou, A. Dai, H. Li, C. Li, X. Chen, J. Lu, J.-S. von Storch, and B. Wu, 2020a: South

760   Asian summer monsoon projections constrained by the Interdecadal Pacific Oscillation.

761   *Science Advances,6, eaay6546*. DOI: 10.1126/sciadv.aay6546.

762   Huang, X., T. Zhou, A. Turner, A. Dai, X. Chen, R. Clark, J. Jiang, W. Man, J. Murphy, J. Rostron, B.

763   Wu, L. Zhang, W. Zhang, and L. Zou, 2020b: The recent decline and recovery of Indian

764   summer monsoon rainfall: relative roles of external forcing and internal variability. *J.*

765   *Climate,* Accepted 12 March 2020. doi: 10.1175/JCLI-D-19-0833.1

766   Huang, X., T. Zhou, W. Zhnag, J. Jiang, P. Li, Y. Zhao, 2019: Northern Hemipshere land monsoon

767   precipitation chnages in the twentieth century revealed by multple Reanalysis datasets,

768   Climate Dyn., https://doi.org/10.1007/s00382-019-04982-z

769   Jalihal, C., J. Srinivasan, and A. Chakraborty, 2019: Modulation of Indian monsoon by water

770   vapor and cloud feedback over the past 22,000 years. *Nature Communications,* **10,** 1–8,

771   doi:10.1038/s41467-019-13754-6.

772   Jiang, X., Y. Luo, D.-L. Zhang, and M. Wu, 2019: Urbanization Enhanced Summertime Extreme

773   Hourly Precipitation over the Yangtze River Delta, J Climate, Accepted.

774   Jiang Jie, Tianjun Zhou. 2019. Global monsoon responses to decadal sea surface temperature

775   variations during the twentieth century: Evidence from AGCM simulations. *Journal of*

776   *Climate*, doi: 10.1175/JCLI-D-18-0890.1

777   Jin, Q., Wang, C. A revival of Indian summer monsoon rainfall since 2002. *Nature Clim*

778   *Change* **7,** 587–594 (2017).

779   Jourdain, N. C., A. S. Gupta, A. S. Taschetto, C. C. Ummenhofer, A. F. Moise, and K. Ashok, 2013:

780   The Indo-Australian monsoon and its relationship to ENSO and IOD in reanalysis data

781   and the CMIP3/CMIP5 simulations. *Climate Dyn.,* **41,** 3073–3102, doi:10.1007/s00382-

782   013-1676-1.Kawase, H., A. Murata, R. Mizuta, H. Sasaki, M. Nosaka, M. Ishii, and I.

783   Takayabu, 2016: Enhancement of heavy daily snowfall in central Japan due to global

784   warming as projected by large ensemble of regional climate simulations. Climatic

785   Change, 139, 265-278, doi:10.1007/s10584-016-1781-3.

786 Kawase, H., Y. Imada, H. Sasaki, T. Nakaegawa, A. Murata, M. Nosaka, and I. Talayabu, 2019:

787   Contribution of historical global warming to local-scale heavy precipitation in western

788   Japan estimated by large ensemble high-resolution simulations. J. Geophys. Res. Atmos.,

789   124, 6093-6103, doi:10.1029/2018JD030155.

790 Kendon, E.J., Stratton, R.A., Tucker, S. *et al.* , 2019: Enhanced future changes in wet and dry

791   extremes over Africa at convection-permitting scale. *Nat Commun* **10,** 1794.

792   https://doi.org/10.1038/s41467-019-09776-9

793 Kirchmeier-Young, M. C., F. W. Zwiers, and N. P. Gillett, 2017: Attribution of Extreme Events in

794   Arctic Sea Ice Extent. *J. Climate,* **30,** 553–571.

795 Kitoh, A., H. Endo, K. Krishna Kumar, I. F. A. Cavalcanti, P. Goswami, and T. Zhou, 2013:

796   Monsoons in a changing world: a regional perspective in a global context. *J. Geophys.*

797   *Res.,* **118,** 3053–3065, doi:10.1002/jgrd.50258.

798 Kitoh, A., 2017: The Asian monsoon and its future change in climate models: a review. *J.*

799   *Meteor. Soc. Japan,* **95,** 7-33, doi:10.2151/jmsj.2017-002.

800 Knutson et al. 2019a: Tropical Cyclones and Climate Change Assessment: Part I. Detection and

801   Attribution. Bull. Amer. Meteorol. Soc. doi.org/10.1175/BAMS-D-18-0189.1

802   Knutson et al. 2019b: Tropical Cyclones and Climate Change Assessment: Part II. Projected

803   Response to Anthropogenic Warming. Bull. Amer. Meteorol. Soc.

804   doi.org/10.1175/BAMS-D-18-0194.1

805   Krishnan, R., T.P. Sabin, D.C. Ayantika, A. Kitoh, M. Sugi, H. Murakami, A.G. Turner, J.M. Slingo

806   and K. Rajendran, 2013: Will the South Asian monsoon overturning circulation stabilize

807   any further? Clim.Dyn., 40, 187–211.

808   Krishnan, R., T. P. Sabin, R. Vellore, M. Mujumdar, J. Sanjay, B. N. Goswami, F. Hourdin, J.-L.

809   Dufresne, and P. Terray, 2016: Deciphering the desiccation trend of the South Asian

810   monsoon hydroclimate in a warming world. *Climate Dyn.,* **47,** 1007–1027.

811   Lahmers, T. M., C. L. Castro, D. K. Adams, Y. L. Serra, J. J. Brost, and T. Luong, 2016: Long-term

812   changes in the climatology of transient inverted troughs over the North American

813   monsoon region and their effects on precipitation. *J. Climate,* **29,** 6037–6064.

814   Lau, W. K.-M., and K.-M. Kim, 2017: Competing influences of greenhouse warming and aerosols

815   on Asian summer monsoon circulation and rainfall, *Asia-Pac., J. Atmos. Sci.,* **53,** 181–

816   194.

817   Lee, J.-Y. and B. Wang, 2014: Future change of global monsoon in the CMIP5. *Climate Dyn.,* **42,**

818   101–119, doi:10.1007/s00382-012-1564-0.

819   Lee, J.-Y., K.-S. Yun, Y.-M. Yang, E.-S. Chung and A. Babu, 2019: Challenges in constraining future

820   change of global land precipitation in CMIP6 models. Presented at the WMO Workshop

821   on Monsoon Climate Change Assessment, 2-3 December 2019, Zhuhai, China.

822   Li, G., S.-P. Xie, Y. Du, and Y. Luo, 2016: Effects of excessive equatorial cold tongue bias on the

823   projections of tropical Pacific climate change. Part I: the warming pattern in CMIP5

824   multi-model ensemble. *Climate Dyn., **47,*** 3817–3831.

825   Li, J., and B. Wang, 2018: Origins of the decadal predictability of East Asian land summer

826   monsoon rainfall. *J. Climate,* **31,** 6229–6243.

827   Li, J., Z. Wu, Z. Jiang, and J. He, 2010: Can global warming strengthen the East Asian summer

828   monsoon? *J. Climate*, **23**, 6696-6705.

829   Li, W., Fu, R., 2006: Influence of cold air intrusions on the wet season onset over Amazonia. *J.*

830   *Climate,* **19,** 257–275, doi:10.1175/JCLI3614.1.

831   Li, X., J. Yu, and Y. Li, 2013: Recent Summer Rainfall Increase and Surface Cooling over Northern

832   Australia since the Late 1970s: A Response to Warming in the Tropical Western Pacific. *J.*

833   *Climate,* **26,** 7221–7239, doi:10.1175/JCLI-D-12-00786.1.

834   Li, Z., W. K. M. Lau, V. Ramanathan, et al., 2016: Aerosol and monsoon climate interactions over

835   Asia. Reviews of Geophysics, 54(1-4), 866-929.

836   Li, Z., Y. Sun, T. Li, Y. Ding, and T. Hu, 2019: Future changes in East Asian summer monsoon

837   circulation and precipitation under 1.5° C to 5° C of warming. *Earth's Future,* accepted.

838   Liebmann, B., M. P. Hoerling, C. Funk, I. Bladé, R. M. Dole, D. Allured, X. Quan, P. Pegion, and J.

839   K. Eischeid, 2014: Understanding recent Horn of Africa rainfall variability and change. *J.*

840   *Climate,* **27**, 8629–8645, doi:10.1175/JCLI-D-13-00714.1.

841   Lin, L., Z. Wang, Y. Xu, Q.Fu, and W. Dong, 2018: Larger Sensitivity of Precipitation Extremes to

842   Aerosol Than Greenhouse Gas Forcing in CMIP5 Models. *J. Geophys. Res. Atmos.,* **123,**

843   8062–8073. doi:10.1029/2018JD028821.

844   Liu, J., B. Wang, Q. H. Ding, X. Y. Kuang, W. Soon, and E. Zorita, 2009: Centennial variations of

845   the global monsoon precipitation in the last millennium: results from ECHO-G model. *J.*

846   *Climate,* **22,** 2356–2371, doi:10.1175/2008JCLI2353.1.

847   Liu, J., B. Wang, M. A. Cane, S.-Y. Yim and J.-Y. Lee, 2013: Divergent global precipitation changes

848   induced by natural versus anthropogenic forcing. *Nature,* **493,** 656–659.

849   Lodoun, T., A. Giannini, P. S. Traoré, L. Somé, M. Sanon, M. Vaksmann, and J. M. Rasolodimby,

850   2013: Changes in seasonal descriptors of precipitation in Burkina Faso associated with

851   late 20th century drought and recovery in West Africa. *Environmental Development,* **5,**

852   96–108.

853   Luong, T. M., C. L. Castro, H.-I Chang, T. Lahmers, D. K. Adams, and C. A. Ochoa-Moya, 2017: The

854   more extreme nature of North American monsoon precipitation in the southwestern

855   U.S. as revealed by a historical climatology of simulated severe weather events. *J. Appl.*

856   *Meteor. Climatol.,* **56,** 2509–2529.

857   Ma, S., T. Zhou, D. A. Stone, D. Polson, A. Dai, P. A. Stott, H. von Storch, Y. Qian, C. Burke, P. Wu,

858   L. Zou, and A. Ciavarella, 2017: Detectable anthropogenic shift toward heavy

859   precipitation over eastern China. J. Climate, 30, 1381-1396.

860   Maher, N. and Coauthors, 2019: The Max Planck Institute Grand Ensemble: Enabling the

861   exploration of climate system variability. *J. Advances in Modeling Earth Systems,* **11,**

862   2050–2069.

863   Maidment, R. I., R. P. Allan, and E. Black, 2015: Recent observed and simulated changes in

864   precipitation over Africa. *Geophys. Res. Lett.,* **42,** 8155–8164,

865   doi:10.1002/2015GL065765.

866   Malhi, Y., J. T. Roberts, R. A. Betts, T. J. Killeen, W. Li, and C. A. Nobre, 2008: Climate change,

867   deforestation, and the fate of the Amazon. *Science,* **319,** 169–172,

868   doi:10.1126/science.1146961.

869   Maloney, E.D., Adames, Á.F. & Bui, H.X. Madden–Julian oscillation changes under

870   anthropogenic warming. *Nature Clim Change* **9,** 26–33 (2019).

871   https://doi.org/10.1038/s41558-018-0331-6

872   Marvel, K., M. Biasutti, and C. Bonfils, 2019: Fingerprints of external forcing agents on Sahel

873   rainfall. *Environ. Res. Lett.,* revised version submitted and available for download in the

874   ESSOAr repository: https://doi.org/10.1002/essoar.10502593.1

875   Moon, S., and K. J. Ha, 2017: Temperature and precipitation in the context of the annual cycle

876   over Asia: Model evaluation and future change. *Asia-Pacific J. Atmos. Sci.,* **53,** 229–242,

877   doi:10.1007/s13143-017-0024-5.

878   Murphy, J. M., B. B. Booth, C. A. Boulton, R. T. Clark, G. R. Harris, J. A. Lowe and D. M. H. Sexton,

879   2014: Transient climate changes in a perturbed parameter ensemble of emissions-

880   driven earth system model simulations. *Climate Dyn.,* **43,** 2855–2885,

881   doi:10.1007/s00382-014-2097-5.

882   Nam, C., S. Bony, J.-L. Dufresne, and H. Chepfer, 2012: The 'too few, too bright' tropical low-

883   cloud problem in CMIP5 models. *Geophys. Res. Lett.,* **39,** L21801.

884   Nguyen, H., A. Evans, C. Lucas, I. Smith, and B. Timbal, 2013: The Hadley circulation in

885   reanalyses: Climatology, variability, and change. *J. Climate,* **26,** 3357–3376.

886   Nicholls, N., C. Landsea, and J. Gill, 1998: Recent trends in Australian region tropical cyclone

887   activity. *Meteorol. Atmos. Phys.,* **65,** 197–205.

888 Nigam, S., Y. Zhao, A. Ruiz-Barradas and T. Zhou, 2015: The South-Flood North-Drought pattern

889   over eastern China and the drying of the Gangetic Plain. Chao. 22 in Climate Change:

890   Multidecadal and Beyond. Eds. C.P. Chang, M. Ghil, M. Latif, J. M. Wallace. World

891   Scientific Series on Asia-Pacific Weather and Climate, Vol. 6, World Scientific, Singapore.

892   347-359. doi: 10.1142/9789814579933_0022.

893 Oh, H., K.-J. Ha, and A. Timmermann, 2018: Disentangling impacts of dynamic and

894   thermodynamic components on late summer rainfall anomailes in East Asia, *J. Geophys.*

895   *Res.,* **123,** 8623–8633, doi:10.1029/2018JD028652.

896 Omondi, P., L. A. Ogallo, R. Anya, J. M. Muthama, J. Ininda, 2013: Linkages between global sea

897   surface temperatures and decadal rainfall variability over Eastern Africa region. *Int. J.*

898   *Climatol.,* **33,** 2082–2104.

899 Panthou, G., T. Vischel, and T. Lebel, 2014: Recent trends in the regime of extreme rainfall in

900   the Central Sahel. *Int. J. Climatol.,* **3,** 3998–4006.

901 Pascale, S., W. R. Boos., S. Bordoni., T. L. Delworth, S. B. Kapnick, H. Murakami1, G. A. Vecchi,

902   and W. Zhang, 2017: Weakening of the North American monsoon with global warming.

903   *Nat. Clim. Change,* **7,** 806–812.

904 Pascale, S., L. M. Carvalho, D. K. Adams, C. L. Castro, and I. F. A. Cavalcanti, 2019: Current and

905   future variations of the monsoons of the Americas in a warming climate, *Curr. Clim.*

906   *Change Rep.,* **5,** 125–144.

907 Polson, D., M. Bollasina, G. C. Hegerl, and L. J. Wilcox, 2014: Decreased monsoon precipitation

908   in the Northern Hemisphere due to anthropogenic aerosols. *Geophys. Res. Lett.,* **41,**

909   6023–6029. doi:10.1002/2014GL060811.

910   Prein, A. F., R. M. Rasmussen, K. Ikeda, C. Liu, M. P. Clark, and G. J. Holland, 2016: The future

911   intensification of hourly precipitation extremes. *Nature Climate Change,* **7,** 48–52.

912   Privé, N. C. and R. A. Plumb, 2007: Monsoon dynamics with interactive forcing. Part I:

913   Axisymmetric studies. *J. Atmos. Sci.,* **64,** 1417–1430.

914   Richardson, T. B., P. M. Forster, T. Andrews, O. Boucher, G. Faluvegid, D. Fläschner, Ø.

915   Hodnebrog, M. Kasoar, A. Kirkevåg, J.-F. Lamarque, G. Myhre, D. Olivié, B. H. Samset, D.

916   Shawki, D. Shindell, T. Takemura, and A. Voulgarakis, 2018: Drivers of precipitation

917   change: An energetic understanding. *J. Climate,* **31,** 9641–9657.

918   Rotstayn, L. D., W. Cai, M. R. Dix, G. D. Farquhar, Y. Feng, P. Ginoux, M. Herzog, A. Ito, J. E.

919   Penner, M. L. Roderick, M. and Wang, 2007: Have Australian rainfall and cloudiness

920   increased due to the remote effects of Asian anthropogenic aerosols? *J. Geophys. Res.,*

921   **112,** D09202, doi:10.1029/2006jd007712.

922   Roxy, M. K., K. Ritika, P. Terray, R. Murtugudde, K. Ashok, and B. N. Goswami, 2015: Drying of

923   Indian subcontinent by rapid Indian Ocean warming and a weakening land-sea thermal

924   gradient. *Nature Communications,* **6,** 7423, doi:10.1038/ncomms8423.

925   Roxy, M. K., Ghosh, S., Pathak, A., Athulya, R., Mujumdar, M., Murtugudde, R., ... & Rajeevan,

926   M., 2017: A threefold rise in widespread extreme rain events over central India. Nature

927   communications, 8, 708.

928   Sabeerali, C., and R. Ajayamohan, 2017: On the shortening of Indian summer monsoon season

929   in a warming scenario. *Climate Dynamics***,** 1-16.

930   Salzmann, M., 2016: Global warming without global mean precipitation increase? *Sci. Adv.,* **2,**

931   e1501572.

932   Salzmann, M., H. Weser, and R. Cherian, 2014: J. Geophys. Res. Atmos. 119, 11321-11337.

933   Salzmann, M., and R. Cherian, 2015: On the enhancement of the Indian summer monsoon

934   drying by Pacific multidecadal variability during the latter half of the twentieth century.

935   J. Geophys. Res. Atmos. 120(18), 9103-9118.

936   Sanogo, S., A. H. Fink, J. A. Omotosho, A. Ba, R. Redl, and V. Ermert, 2015: Spatio-temporal

937   characteristics of the recent rainfall recovery in West Africa. *Int. J. Climatol.,* **35,** 4589–

938   4605.

939   Sarr, M. A., M. Zoromé, O. Seidou, C. R. Bryant, and P. Gachon, 2013: Recent trends in selected

940   extreme precipitation indices in Senegal–A changepoint approach. *J. Hydrology,* **505,**

941   326–334.

942   Seth, A., S. A. Rauscher, M. Biasutti, A. Giannini, S. J. Carmargo and M. Rojas, 2013: CMIP5

943   projected changes in the annual cycle of precipitation in monsoon regions. *J. Climate,*

944   **26,** 7328–7351, doi:10.1175/JCLI-D-12-00726.1.

945   Sharmila, S., S. Joseph, A. Sahai, S. Abhilash, and R. Chattopadhyay, 2015: Future projection of

946   Indian summer monsoon variability under climate change scenario: An assessment from

947   CMIP5 climate models. *Global and Planetary Change,* **124,** 62–78.

948   Shawki, D., Voulgarakis, A. , Chakraborty, A., Kasoar, M., and J. Srinivasan, 2018: The South

949   Asian monsoon response to remote aerosols: Global and regional mechanisms, *J.*

950   *Geophys. Res*., *Atmospheres,* 123, 11, 585–11,601.

951   Shi., H., B. Wang, Cook, E. D., J. Liu, and F. Liu, 2018: Asian Summer Precipitation over the Past

952   544 Years Reconstructed by Merging Tree Rings and Historical Documentary Records**.** *J.*

953   *Climate*, 31, 7845-7861. DOI: 10.1175/JCLI-D-18-0003.1.

954 Shonk, J. P., A. G. Turner, A. Chevuturi, L. Wilcox, A. J. Dittus, and E. Hawkins, 2019: Uncertainty

955 in aerosol radiative forcing impacts the simulated global monsoon in the 20th century.

956 *Geophys. Res. Letts.,* revised version submitted. The latest version of this paper can be

957 accessed at https://livereadingac-

958 my.sharepoint.com/:f:/g/personal/a_g_turner_reading_ac_uk/

959 El8hjGgHjs5KooEbLEP0lIIBGgSajLIwumjN9ARCV7lJNQ?e=GrH4NI.

960 Singh, M. S., Z. Kuang, and Y. Tian, 2017: Eddy inuences on the strength of the Hadley

961 circulation: Dynamic and thermodynamic perspectives. *J. Atmos. Sci.,* **74,** 467–486.

962 Singh, D., S. Ghosh, M. K. Roxy, and S. McDermid, 2019: Indian summer monsoon: Extreme

963 events, historical changes, and role of anthropogenic forcings. *WIREs Clim. Change*,

964 e571, doi:10.1002/wcc571.

965 Sigmond, M., and J. C. Fyfe, 2016: Tropical Pacific impacts on cooling North American winters.

966 *Nature Climate Change,* **6,** 970–974.

967 Skansi, M. M., M. Brunet, J. Sigró, E. Aguilar, J. A. A. Groening, O. J. Bentancur, Y. R. C. Geier, R.

968 L. C. Amaya, H. Jácome, A. M. Ramos, C. O. Rojas, A. M. Pasten, S. S. Mitro, C. V.

969 Jiménez, R. Martínez, L. V. Alexander, P.D. Jones, 2013: Warming and wetting signals

970 emerging from analysis of changes in climate extreme indices over South America.

971 *Global and Planetary Change*, 100, 295-307. doi:10.1016/j.gloplacha.2012.11.004.

972 Sobel, A. H., and J. D. Neelin, 2006: The boundary layer contribution to intertropical

973 convergence zones in the quasi-equilibrium tropical circulation model framework.

974 *Theor. Comput. Fluid Dyn.,* **20,** 323–350.

975   Sontakke NA, Singh N, Singh HN (2008) Instrumental period rainfall series of the Indian region

976   (AD 1813-2005): Revised reconstruction, update and analysis. Holocene 18:1055–1066.

977   https://doi.org/10.1177/0959683608095576

978   Sooraj, K., P. Terray, and P. Xavier, 2016: Sub-seasonal behaviour of Asian summer monsoon

979   under a changing climate: Assessments using CMIP5 models. *Climate Dyn.*, **46,** 4003–

980   4025.

981   Sperber, K. R., H. Annamalai, I.-S. Kang, A. Kitoh, A. Moise, A. Turner, B. Wang, and T. Zhou,

982   2013: The Asian summer monsoon: an intercomparison of CMIP5 vs. CMIP3 siulations of

983   the late 20th century. CLim. Dyn., 41, 2711-2744.

984   Taylor, C. M., D. Belušic, F. Guichard, D. J. Parker, T. Vischel, O. Bock, P. P. Harris, S. Janicot, C.

985   Klein, and Panthou, G., 2017: Frequency of extreme Sahelian storms tripled since 1982

986   in satellite observations. *Nature,* **544,** 475–478.

987   Taylor, C. M., A. H. Fink, C. Klein, D. J. Parker, F. Guichard, P. P. Harris, and K.R. Knapp, 2018:

988   Earlier seasonal onset of intense mesoscale convective systems in the Congo Basin since

989   1999. *Geophys. Res. Lett.,* **45,** 13458–13467, doi:10.1029/2018GL080516.

990   Timbal, B. and W. Drosdowsky, 2013: The relationship between the decline of South Eastern

991   Australia rainfall and the strengthening of the sub-tropical ridge. *Int. J. Clim.,* **33,** 1021–

992   1034.

993   Turner, A. G., G. S. Bhat et al., 2019: Interaction of Convective Organisation with Monsoon

994   Precipitation, Atmosphere, Surface and Sea: the 2016 INCOMPASS field campaign in

995   India. *Quarterly Journal of the Royal Meteorological Society*, doi: 10.1002/qj.3633.

996   Vera, C. S., and L. Diaz, 2015: Anthropogenic influence on summer precipitation trends over

997   South America in CMIP5 models. *Int. J. Climatol.*, **35,** 3172–3177, doi:10.1002/joc.4153.

998   Wang, B., and Q. Ding, 2006: Changes in global monsoon precipitation over the past 56

999   years. Geophys. Res. Lett., 33, L06711, doi: 10.1029/2005GL025347.

1000   Wang, B., and Q. Ding, 2008: Global monsoon: Dominant mode of annual variation in the

1001   tropics. *Dynamics   of   Atmos.   and   Ocean,   special   issue   2,* doi:

1002   10.1016/j.dynatmoce.2007.05.002.

1003   Wang, B., C. Jin, and J. Liu, 2019: Future change of global monsoon projected by CMIP6 models.

1004   *J Climate*, Revised version submitted.

1005   Wang, B., Liu J, Kim HJ, Webster PJ, and Yim SY, 2012: Recent Change of the Global Monsoon

1006   Precipitation (1979-2008). *Climate Dyn..*,39, 1123-1135, doi: 10.1007/s00382-011-1266-

1007   z.

1008   Wang, B., J. Liu, H.-J. Kim, P. J. Webster, S.-Y. Yim, and B. Xiang, 2013: Northern Hemisphere

1009   summer monsoon intensified by mega-El Nino/southern oscillation and Atlantic

1010   multidecadal oscillation. *Proc. Nat. Acad. Sci.,* **110,** 5347–5352.

1011   Wang, B., S-Y. Yim, J.-Y. Lee, J. Liu, and K.-J. Ha, 2014: Future change of Asian-Australian

1012   monsoon under RCP 4.5 anthropogenic warming scenario. *Climate Dyn.,* **42,** 83–100.

1013   Wang, B., J. Li, M.A. Cane, J. Liu, P.J. Webster, B. Xiang, H.-M. Kim, J. Cao, and K.-J. Ha,

1014   2018: Toward predicting changes in land monsoon rainfall a decade in advance. *J.*

1015   *Climate,* **31,** 2699–2714.

1016   Wang, P.-X., B. Wang, H. Cheng, J. Fasullo, Z. T. Guo, T. Kiefer, Z. Y. Liu, 2014: The Global

1017   Monsoon across Time Scales: Is there coherent variability of regional

1018   monsoons? Climate of the Past., 10, 2163-2291.

1019   Wang, P.-X., B. Wang, H. Cheng, J. Fasullo, Z. Guo, T. Kiefer, and Z. Liu, 2017: The Global

1020   Monsoon across Time Scales: Mechanisms and Outstanding Issues. Earth Science

1021   Reviews, 174, 82-121.

1022   Willetts, P. D., J. H. Marsham, C. E. Birch, D. J. Parker, S. Webster, and J. Petch, 2017: Moist

1023   convection and its upscale effects in simulations of the Indian monsoon with explicit and

1024   parametrized convection. *Q. J. R. Meteorol. Soc.,* 143, 1073-1085, doi:10.1002/qj.2991.

1025   Wright, J. S., R. Fu, J. R. Worden, S. Chakraborty, N. E. Clinton, C. Risi, Y. Sun and L. Yin,

1026   2017: Rainforest-initiated wet season onset over the southern Amazon. *Proceedings of*

1027   *the National Academy of Sciences*, 114(32).

1028   Wu, M., Y. Luo, F. Chen, and W. K. Wong, 2019: Observed link of extreme hourly precipitation

1029   changes to urbanization over coastal South China. J. Appl. Meteor. Climatol., 58, 1799-

1030   1819, doi:10.1175/JAMC-D-18-0284.1.

1031   Yang, Y., L. M. Russell, S. Lou, H. Liao, J. Guo, Y. Liu, B. Singh, and S. J. Ghan, 2017: Dust-wind

1032   interactions can intensify aerosol pollution over eastern China. *Nature Communications,*

1033   **8,** 15333, doi:10.1038/ncomms15333.

1034   Yin, L., R. Fu, E. Shevliakova, and R. E. Dickinson, 2013: How well can CMIP5 simulate

1035   precipitation and its controlling processes over tropical South America? *Climate Dyn.,*

1036   **41,** 3127–3143, doi:10.1007/s00382-012-1582-y.

1037 Ying, J., P. Huang, T. Lian, and H. Tan, 2019: Understanding the effect of an excessive cold

1038   tongue bias on projecting the tropical Pacific SST warming pattern in CMIP5 models.

1039   *Climate Dyn.,* **52,** 1805–1818.

1040 Yuan, X., S. Wang, and Z.-Z. Hu 2018: Do climate change and El Niño increase likelihood of

1041   Yangtze River extreme rainfall? [in "Explaining Extreme Events of 2016 from a Climate

1042   Perspective"]. Bull. Amer. Meteor. Soc., 99 (1), S113-S117. doi: 10.1175/BAMS-D-17-

1043   0089.1.

1044 Zelinka,M. D., T. A. Myers, D. T. McCoy, S. Po-Chedley, P. M. Caldwell , P. Ceppi, S. A. Klein , and

1045   K. E. Taylor, 2020: Causes of higher climate sensitivity in CMIP6 models. Geophysical

1046   Research Letter, 47, e2019GL085782.

1047 Zhang, W., T. Zhou, L. Zhang, and L. Zou, 2019: Future intensification of the water cycle with an

1048   enhanced annual cycle over global land monsoon regions. *J. Climate*, **32,** 5437–5452.

1049 Zhang, W., T. Zhou, L. Zou, L. Zhang, and X. Chen, 2018: Reduced exposure to extreme

1050   precipitation from 0.5°C less warming in global land monsoon regions. Nat. Commun.,

1051   https://doi.org/10.1038/s41467-018-05633-3.

1052 Zhang, W., Zhou, T. 2019: Significant increases in extreme precipitation and the associations

1053   with global warming over the global land monsoon regions. Journal of Climate,

1054   https://doi.org/10.1175/JCLI-D-18-0662.1.

1055 Zheng, F., J. P. Li, and T. Liu, 2014: Some advances in studies of the climatic impacts of the

1056   Southern Hemisphere annular mode. J. Meteor. Res., 28, 820-835.

1057   Zhou, T., D. Gong, J. Li, and B. Li, 2009: Detecting and understanding the multi-decadal

1058   variability of the East Asian Summer Monsoon – Recent progress and state of affairs.

1059   *Meteorologische Zeitschrift,* **18,** 455–467.

1060   Zhou, L. M., Y. H. Tian, R. B. Myneni, P. Ciais, S. Saatchi, Y. Y. Liu, S. L. Piao, H. S. Chan, E. F.

1061   Vermote, and co-authors, 2014: Widespead decline of Congo rainforest greenness in the

1062   past decade. *Nature,* **509,** 86–89, doi:10.1038/nature13265.

1063   Zhou, T., J. Lu and W. Zhang, 2020a: The sources of uncertainty in the projection of global land

1064   monsoon precipitation. *Geophys. Res. Lett.,* under review. Pdf file available at:

1065   https://drive.google.com/open?id=1hkuL4G_xQ-2B6PBYGSMHXDhBrcAARaPZ.

1066   Zhou T., W. Zhang, L. Zhang, X. Zhang, Y. Qian, D. Peng, S. Ma, B. Dong, 2020b: The dynamic

1067   and thermodynamic processes dominating the reduction of global land monsoon

1068   precipitation driven by anthropogenic aerosols emission. *Science China: Earth Sciences*,

1069   accepted and in press.

1070   Zhu, C. W., B. Wang, W. H. Qian, and B. Zhang, 2012: Recent Weakening of Northern East Asian

1071   Summer Monsoon: A Possible Response to Global Warming. *Geophys. Res. Lett.,* **39,**

1072   L09701, doi: 10.1029/2012GL051155.

1073
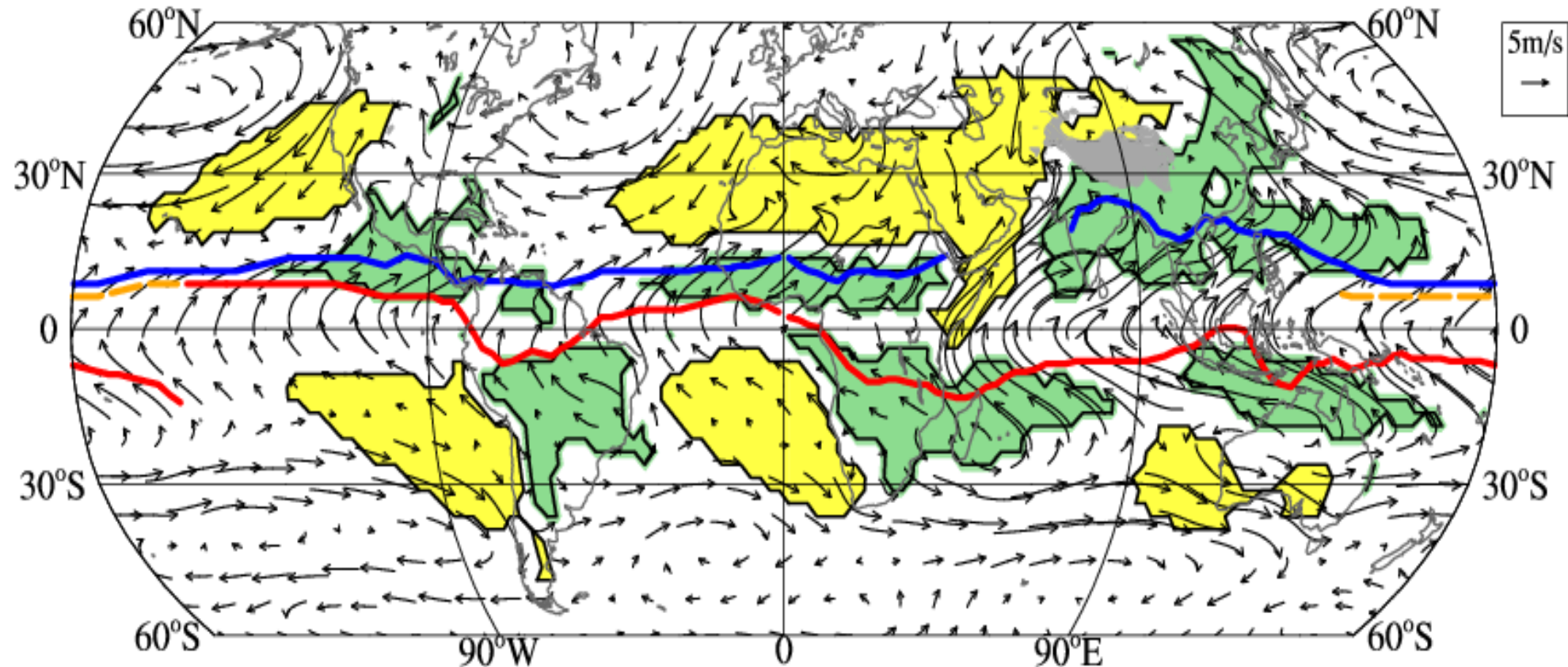
Figure 1. The GM precipitation domain (in Green) defined by the local summer-minus-winter precipitation rate exceeds 2 mm day^{-1}, and the local summer precipitation exceeds 55 % of the annual total (Wang and Ding 2008). Summer denotes May through September for the North ern Hemisphere and November through March for the Southern Hemisphere. The dry regions (in yellow) is defined by local summer precipitation being less than 1 mm day^{-1}. The arrows show August-minus-February 925 hPa winds. The blue (red) lines indicate the ITCZ position in August (February). Adopted from P.X. Wang et al. (2014).
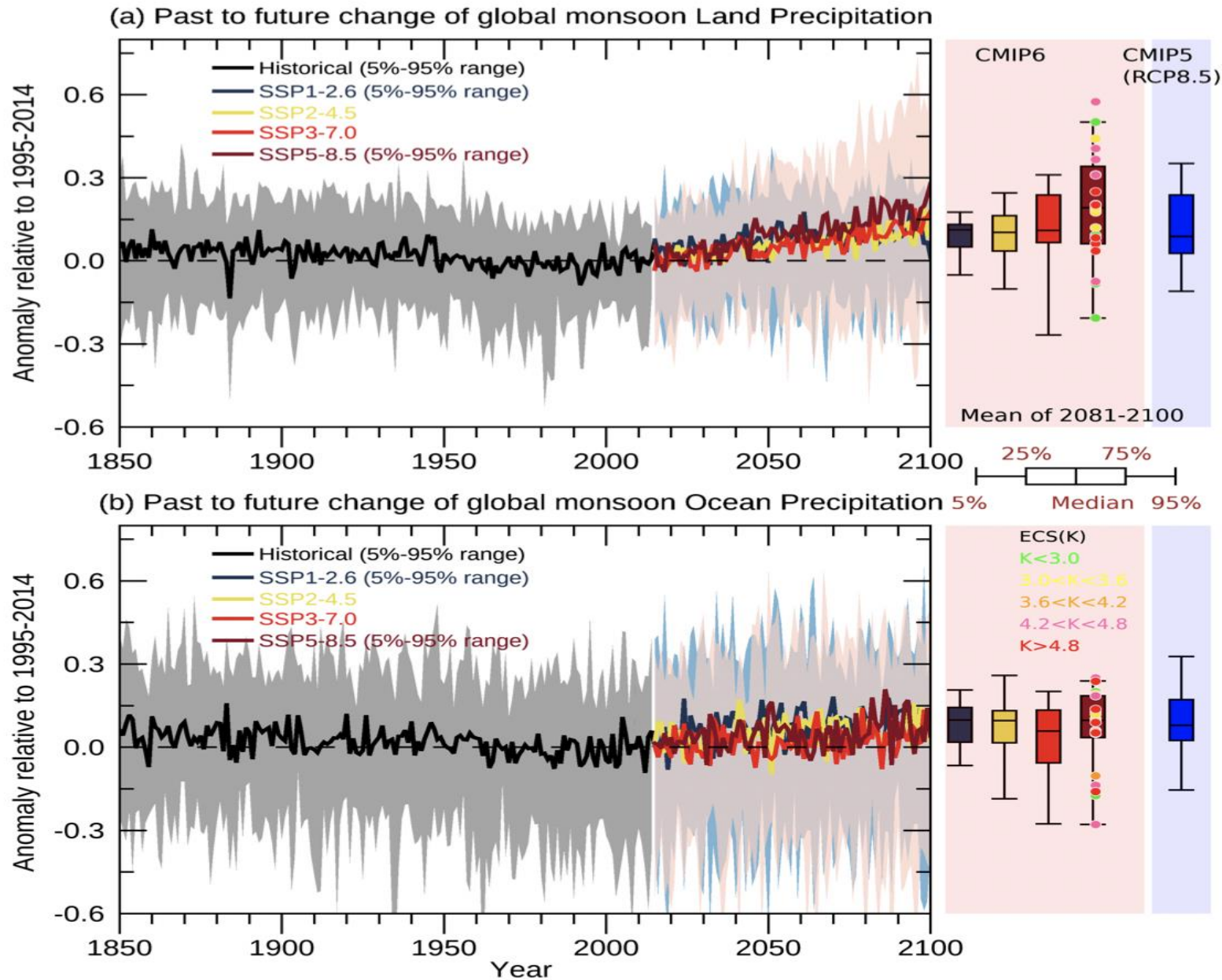
Fig. 2 Past to future changes of annual-mean global monsoon precipitation (mm/day) over (a) land and (b) ocean relative to the recent past (1995-2014) in historical simulation (1850-2014) and four core SSPs (2015-2100) obtained from 34 CMIP6 models. Pink and mid-blue shading indicate 5%-95% likely range of precipitation change in low emission (SSP1-2.6) and high emission (SSP5-8.5) scenario, respectively. The mean change during 2081-2100 relative to the recent past is also shown with the box plot in right-hand side obtained from four SSPs in 34 CMIP6 models compared to RCP 8.5 in 40 CMIP5 models. The solid dot in the box plot for SSP5-8.5 indicates individual model's equilibrium climate sensitivity (ECS).
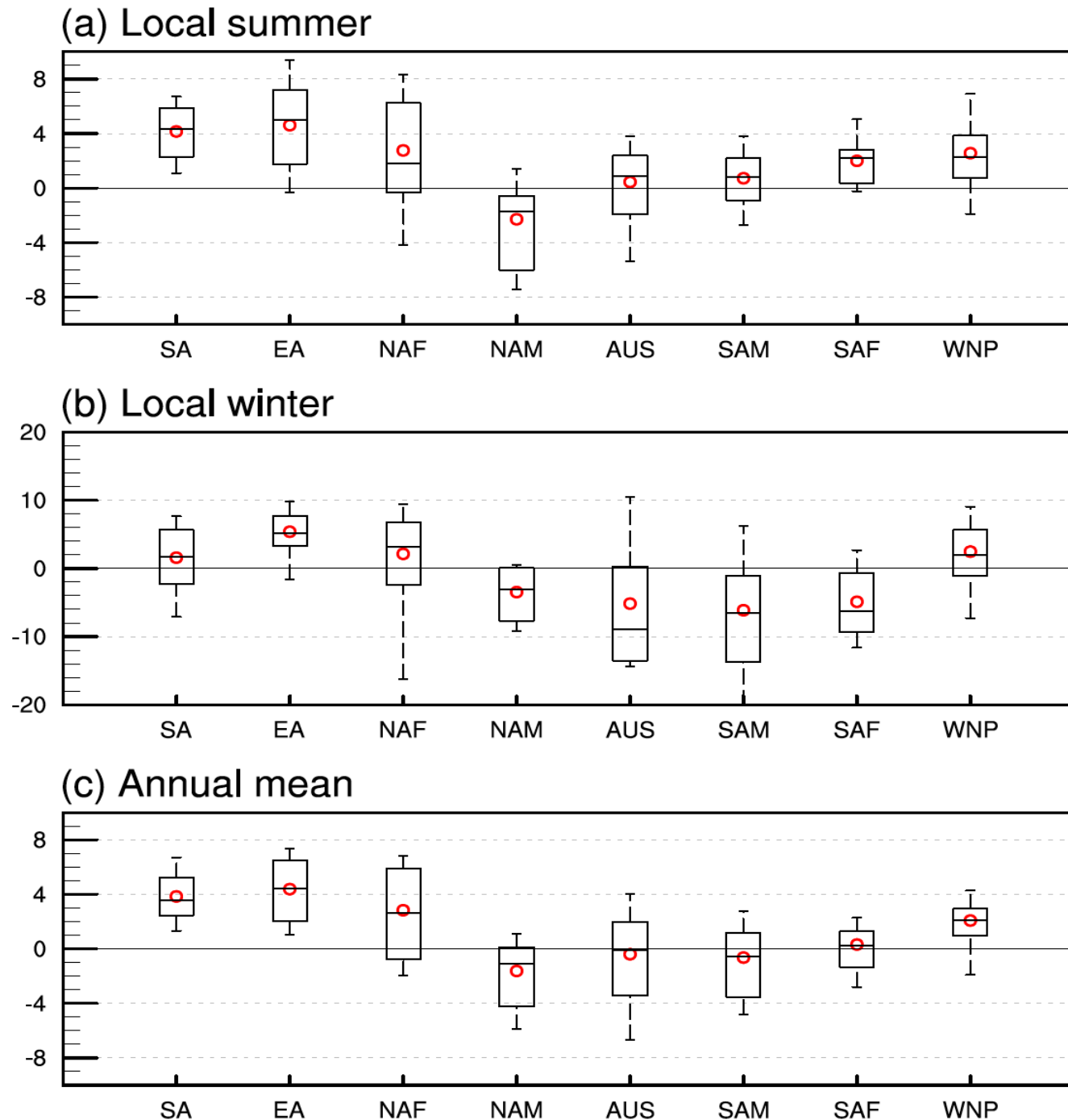
Fig. 3 Projected regional land monsoon precipitation sensitivity under the SSP2-4.5, i. e., the percentage change (2065–2099 relative to 1979–2013) per 1°C global warming, in units of %/°C) derived from 24 CMIP6 models for (a) local summer, (b) local winter, and (c) annual mean land monsoon precipitation for each region. Local summer means JJAS in NH and DJFM for SH, and local winter means the opposite. The upper edge of the box represents the 83th percentile and the lower edge is the 17th percentile, the box contains 66% of the data. The horizontal line within the box is the median. Red circle is the mean. The vertical dash line segments represent the range of nonoutliers (5%-95%).
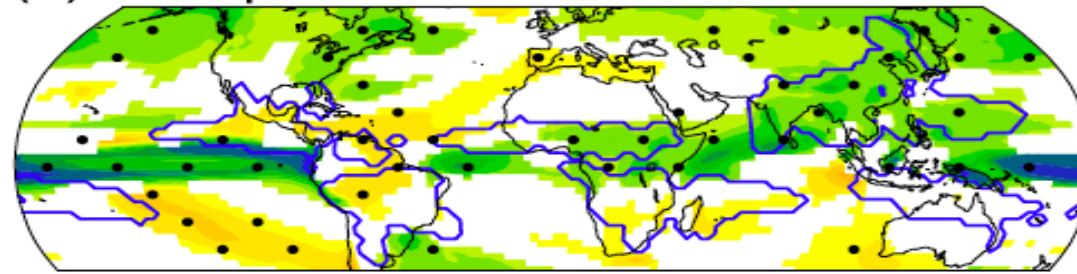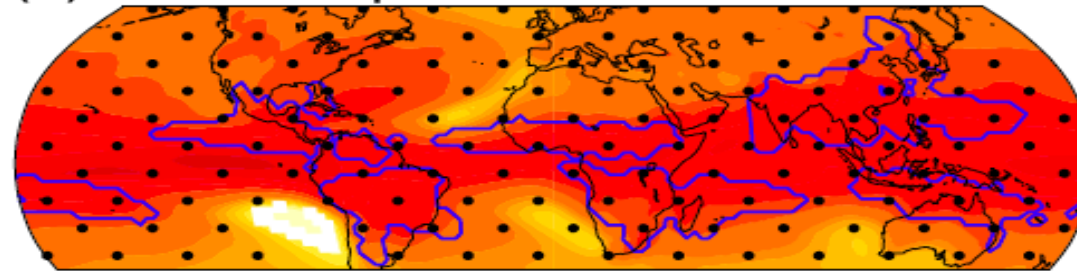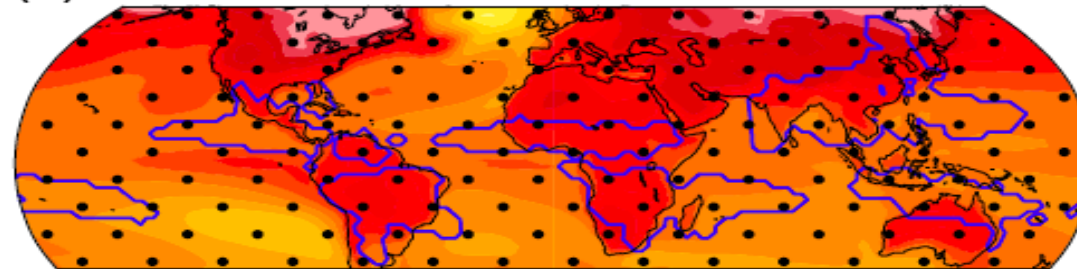
Fig. 4 Changes in the annual mean (a) precipitation, (b) 850 hPa specific humidity, and (c) surface air temperature. Changes are measured by the SSP2-4.5 projection (2065–2099) relative to the historical simulation (1979–2013) in the 15 models' MME. The color shaded region denotes the changes are statistically significant at 66% confidence level (likely change). Stippling denotes areas where the significance exceeds 95% confidence level (very likely) by student t-test.
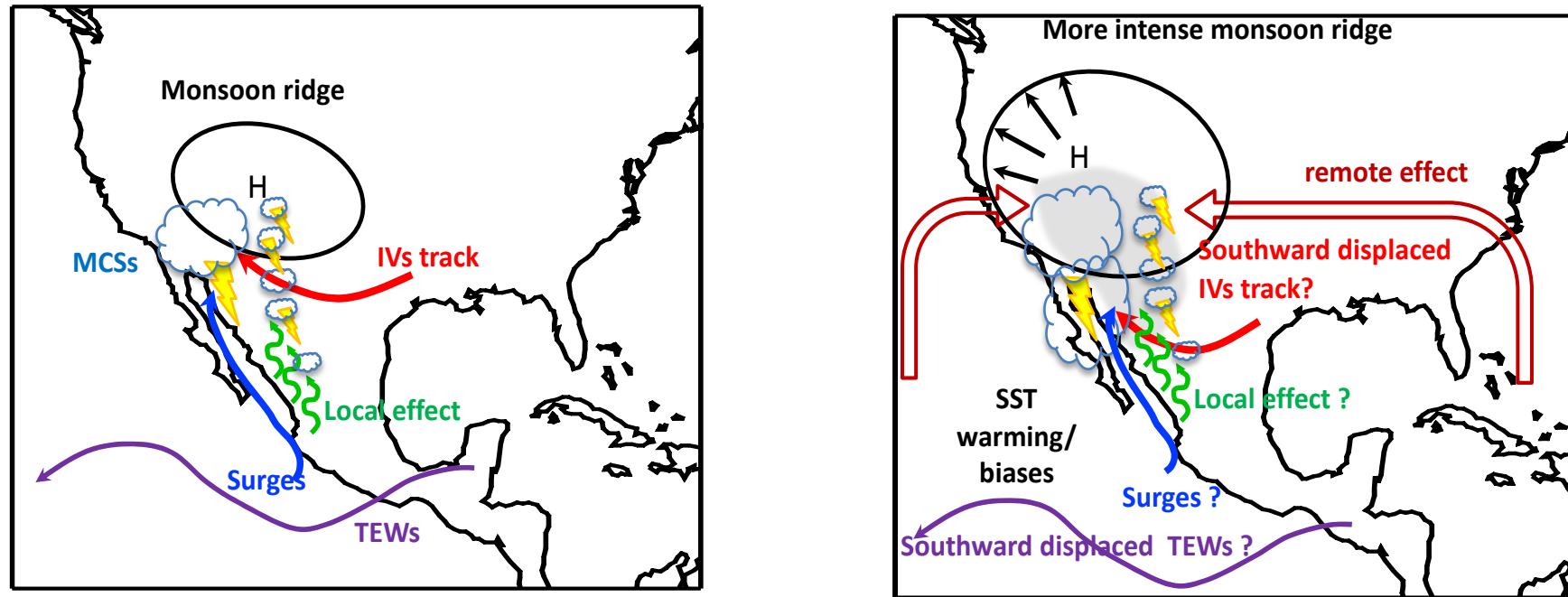
Fig. 5: Schematic main features related to present (left panel) and future (right panel) changes for the North American Monsoon (left). The expansion and northwestward shift of the NAM ridge, the southward shift of the upper-level inverted troughs (IVs) track, and the strengthening of the remote stabilizing effect due to SST warming are shown. Red and blue shading indicates drying and wettening respectively due to the large- scale shifts. Larger clouds in the lower panel is suggestive of more intense MCS-type convection. A question mark (?) on the lower panels indicates uncertainty in the response, as it is the case, for example, for the local mechanisms associated with atmosphere-land interaction, NAM moisture surges and southward shift the tropical easterly waves (TEWs) track.
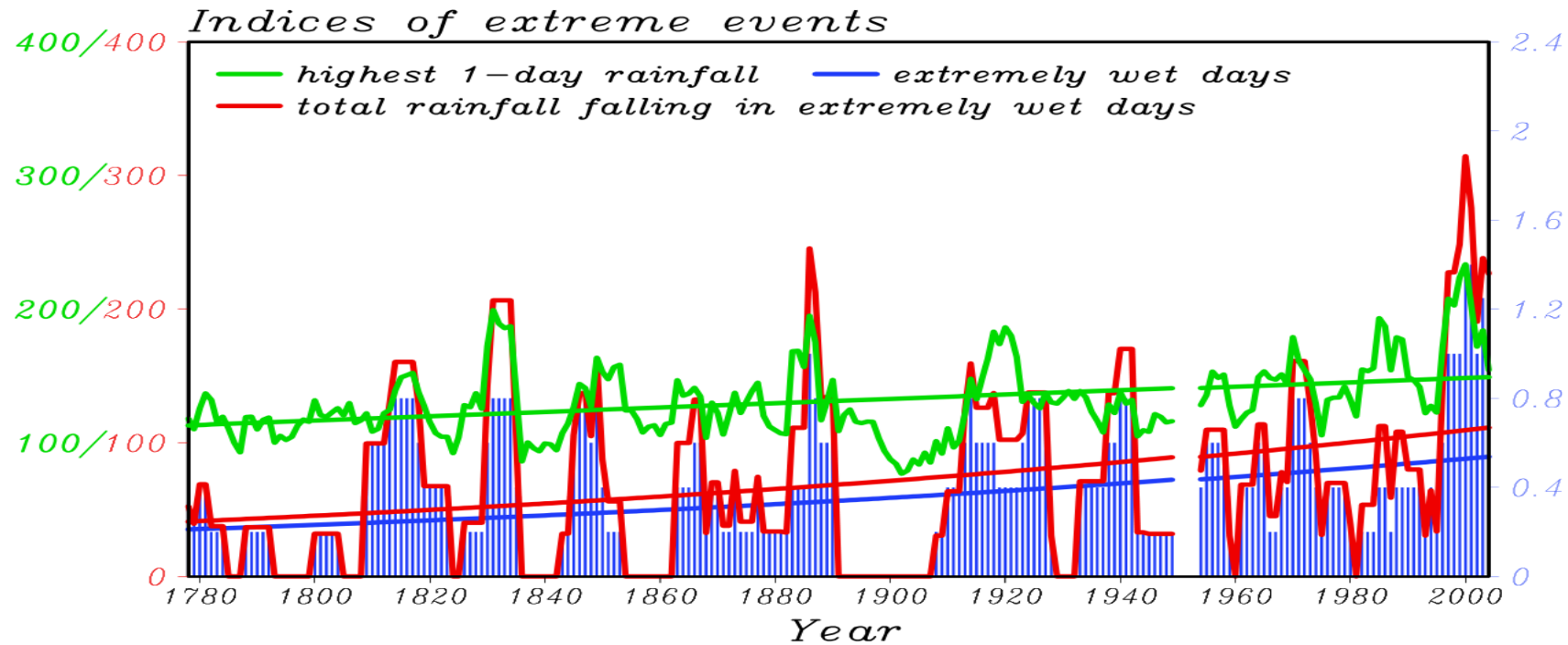
Figure 6. Time series of extreme precipitation events observed at Seoul, Korea since 1778. Running five-year means of the summer highest one-day precipitation amount (green, mm/day in the left y-axis), the number of extremely wet days (blue, right y-axis) and the precipitation amount falling in the extremely wet days (red, mm/day in the left axis). The extremely wet days are calculated as the 99th percentile of the distribution of the summer daily precipitation amount in the 227-year period. Also shown are the corresponding trends obtained by least-square regression for the green curve and logistic regression for the blue and red curve. Adopted from Wang et al. (2006)
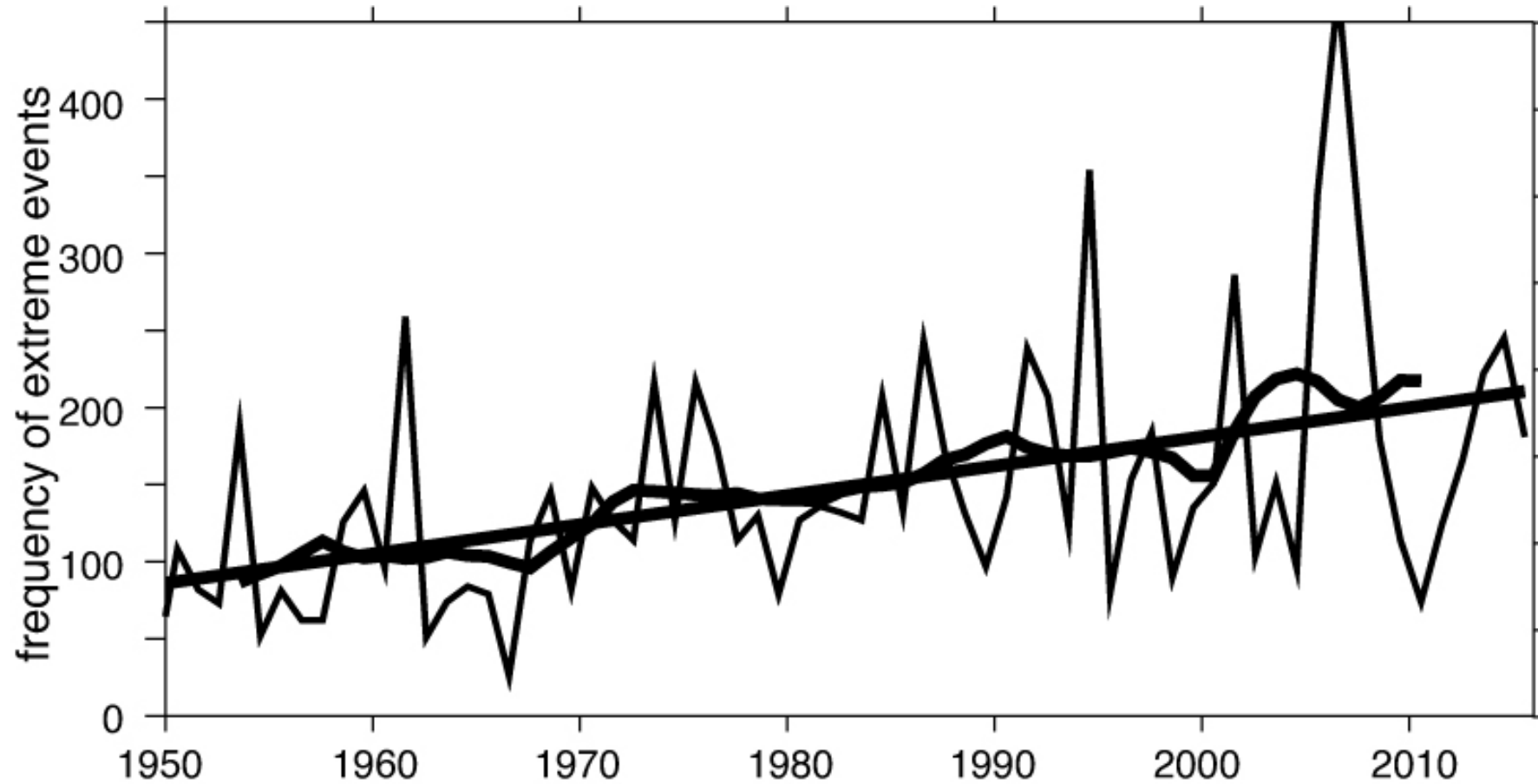
Figure 7. Frequency of extreme rain events (number of grid cells exceeding 150 mm/day per year) over central Indian subcontinent (75°–85° E, 19°–26° N) for the summer monsoon (June-September) during 1950–2015. The trend lines shown in the figures are significant at 95% confidence level. The smoothed curves on the time series analyses represent 10-year moving averages. Adopted from Roxy et al. (2017).
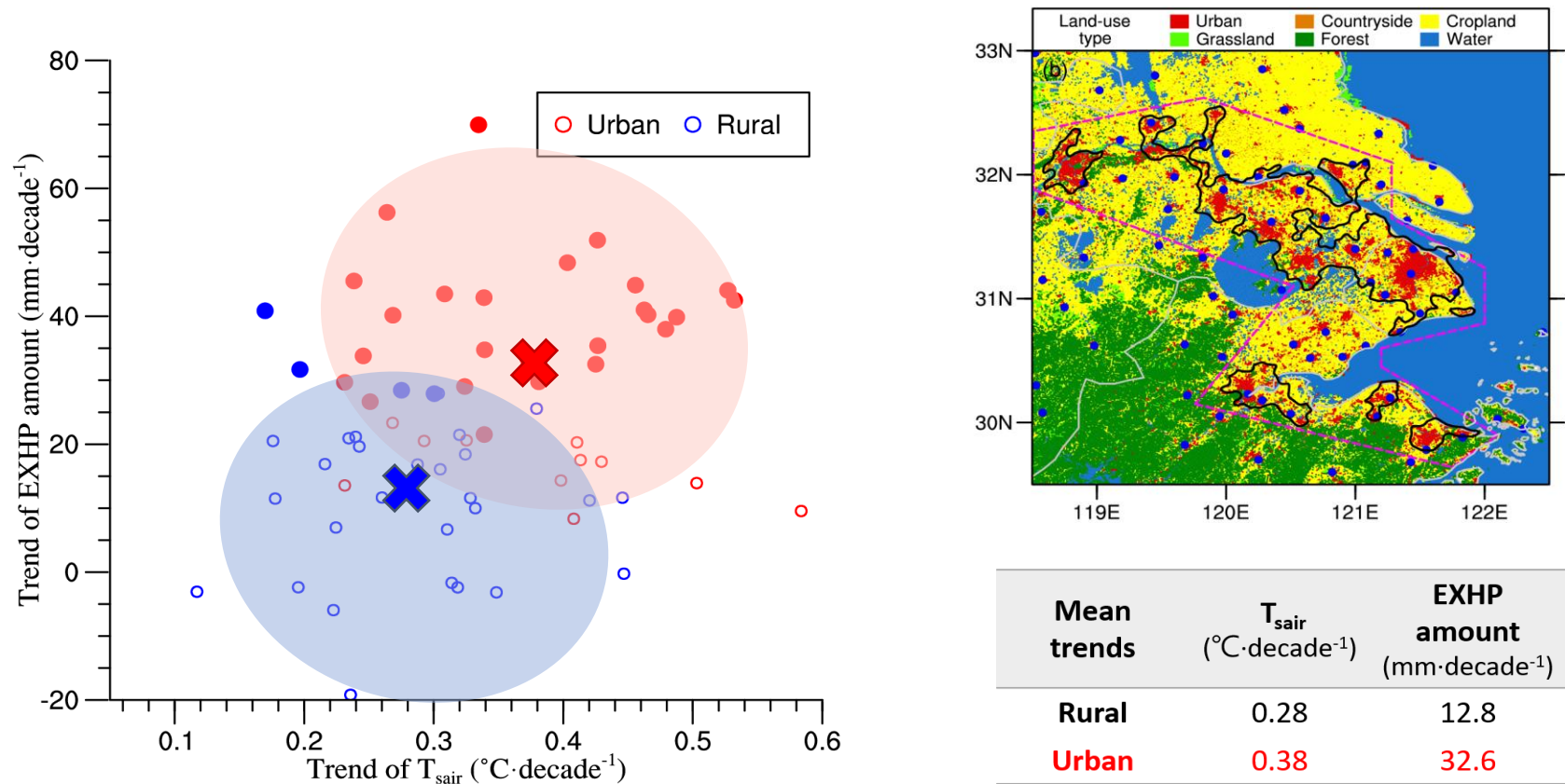
Figure 8 The surface air temperature and extremely hourly rainfall trends for urban stations (red) and rural stations (blue) in the Yangzi River Delta, calculated from changes from 1975-1996 to 1997-2018, during MJJAS. The thick crosses are averages of the station values. Adapted from Figs. 1 and 11 in Jiang et al. (2020)
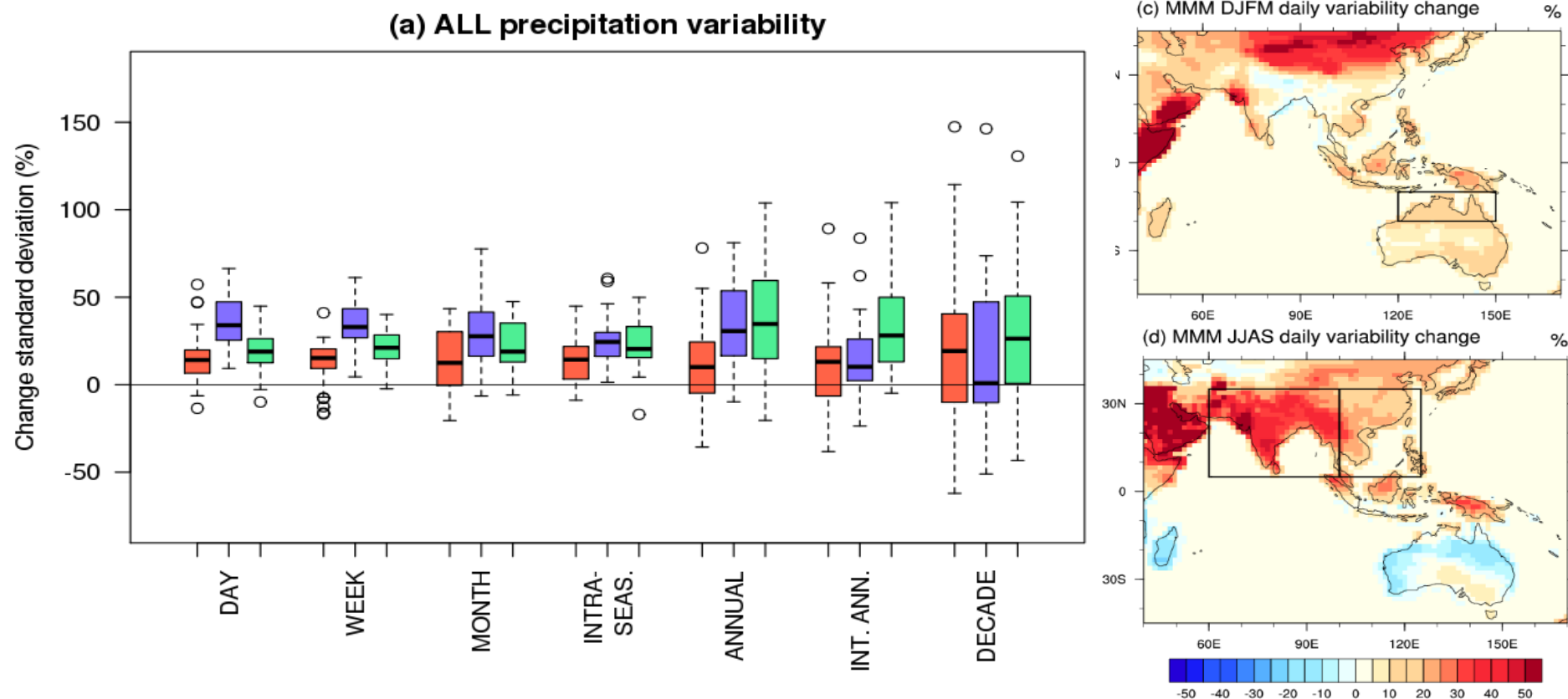
Fig. 9 (a) RCP8.5 (2050-2100) minus HIST (1950-2000) differences in band-pass-filtered daily rainfall standard deviation (%) for Australian (red, left boxes), South Asian (purple, center boxes) and East Asian (green, right boxes) monsoon domain. Data are DJFM months for AUS and JJAS months for SA and EA. Daily data are band-pass-filtered for the set of bands indicated on the x-axis. (c) and (d) are the multi-model mean change in standard deviation of *daily* rainfall (%) from HIST (1950-2000) to RCP8.5 (2050-2100) in (c) DJFM and (d) JJAS. The South Asian (SA), East Asian (EA) and Australian (AUS) monsoon domains are shown in the relevant wet season. (from Brown et al. 2017).